Journal of South American Earth Sciences 52 (2014) 234–259

Contents lists available at ScienceDirect

Journal of South American Earth Sciences

journal homepage: www.elsevier.com/locate/jsames

Tectonic controls on the evolution of the Andean Cenozoic foreland basin: Evidence from fluvial system variations in the Payogastilla Group, in the Calchaquí, Tonco and Amblayo Valleys, NW Argentina

Claudia Inés Galli [a,b,*], Beatriz Coira [c], Ricardo Alonso [d], James Reynolds [e], Massimo Matteini [f], Natalia Hauser [f]

[a] Facultad de Ingeniería, Universidad Nacional de Jujuy, S.S. de Jujuy, Argentina
[b] Facultad de Ciencias Naturales, Universidad Nacional de Salta, Salta, Argentina
[c] CONICET, Instituto de Geología y Minería, Av. Bolivia 1661, S.S. de Jujuy, Argentina
[d] Universidad Nacional de Salta, CONICET, Campo Castañares, 4400 Salta, Argentina
[e] Division of Science and Math, Brevard College, Brevard, NC 28712, USA
[f] Laboratorio de Geocronologia, Instituto de Geociências, Universida de Brasilia, Brazil

ARTICLE INFO

Article history:
Received 11 October 2013
Accepted 19 March 2014

Keywords:
Payogastilla Group
Foreland basin
Sequence stratigraphic
Paleoenviromental
Fluvial system

ABSTRACT

The stratigraphic and sedimentological characteristics of the Payogastilla Group represent important tectono-sedimentary constraints on the evolution of the Andean foreland basin in northwestern Argentina. This nonmarine unit unconformably rests on top of the post-rift deposits of the middle Eocene Lumbrera Formation of the Santa Bárbara Subgroup (Salta Group). Eocene-Pliocene paleoenvironmental changes are a direct result of the tectonic settings and accommodation space. Sequential stratigraphic analysis of the paleoenvironment of the Los Colorados Formation strata indicates the presence of three third-order sequences. Each sequence comprises a low-accommodation systems tract (LAST) and a high-accommodation systems tract (HAST). Substantial tectonic activity from the middle to upper Miocene is represented by Angastaco Formation strata that contain a shallow, gravel-braided fluvial system associated with gravity flows, with thicknesses of 4550 m (Calchaquí River) to 1500 m (Tonco). This activity marked the depocenter of the Angastaco basin. The development of a basal unconformity and the erosion of the Los Colorados Formation suggest a renewed uplift of the source area. Changes in the fluvial systems indicate an increase of the accommodation space.

To obtain better temporal constraints on the basin evolution, new U–Pb ages on zircons from five pyroclastic airfall and two sedimentary levels were determined. A substantial environmental change in the upper Miocene (10–5 Ma) is associated with three episodes of tectonic uplift that are reflected in variations in the sedimentation rates of the Palo Pintado Formation. A reactivated Pliocene tectonic uplift is recorded in alluvial fans that originated from the east.

1. Introduction

Foreland basins form behind continental-margin arc systems and are filled mainly with clastic terrigenous sediments derived from a fold-thrust belt behind the arc. Conspicuous characteristics of this system include the syntectonic character of the sediments and the progressive involvement of the proximal basin margin in the propagating fold-thrust belt (Graham et al., 1986; Condie, 2003). The thick, well-exposed clastic sedimentary accumulations of the Payogastilla Group (Diaz and Malizzia, 1983; Jordan and Alonso, 1987), in northwestern Argentina (Fig. 1) are an excellent example of Cenozoic foreland basin deposits that are associated with the Andean orogeny.

From the base to the top, the Payogastilla Group is composed of the Los Colorados, Angastaco, Palo Pintado, and San Felipe Formations. The strata accumulated in a foreland basin, whose morphology resulted directly from the tectonic inversion of rift basin deposits of the Cretaceous-Paleocene Salta Group (Salfity and Marquilas, 1994). The accumulation of the basal deposits of the

* Corresponding author. Facultad de Ingeniería, UNJu, Av. Bolivia 1551, S.S. de Jujuy, Facultad de Ciencias Naturales, UNSa, Salta, Argentina.
E-mail address: claudiagalli@fibertel.com.ar (C.I. Galli).

http://dx.doi.org/10.1016/j.jsames.2014.03.003
0895-9811/

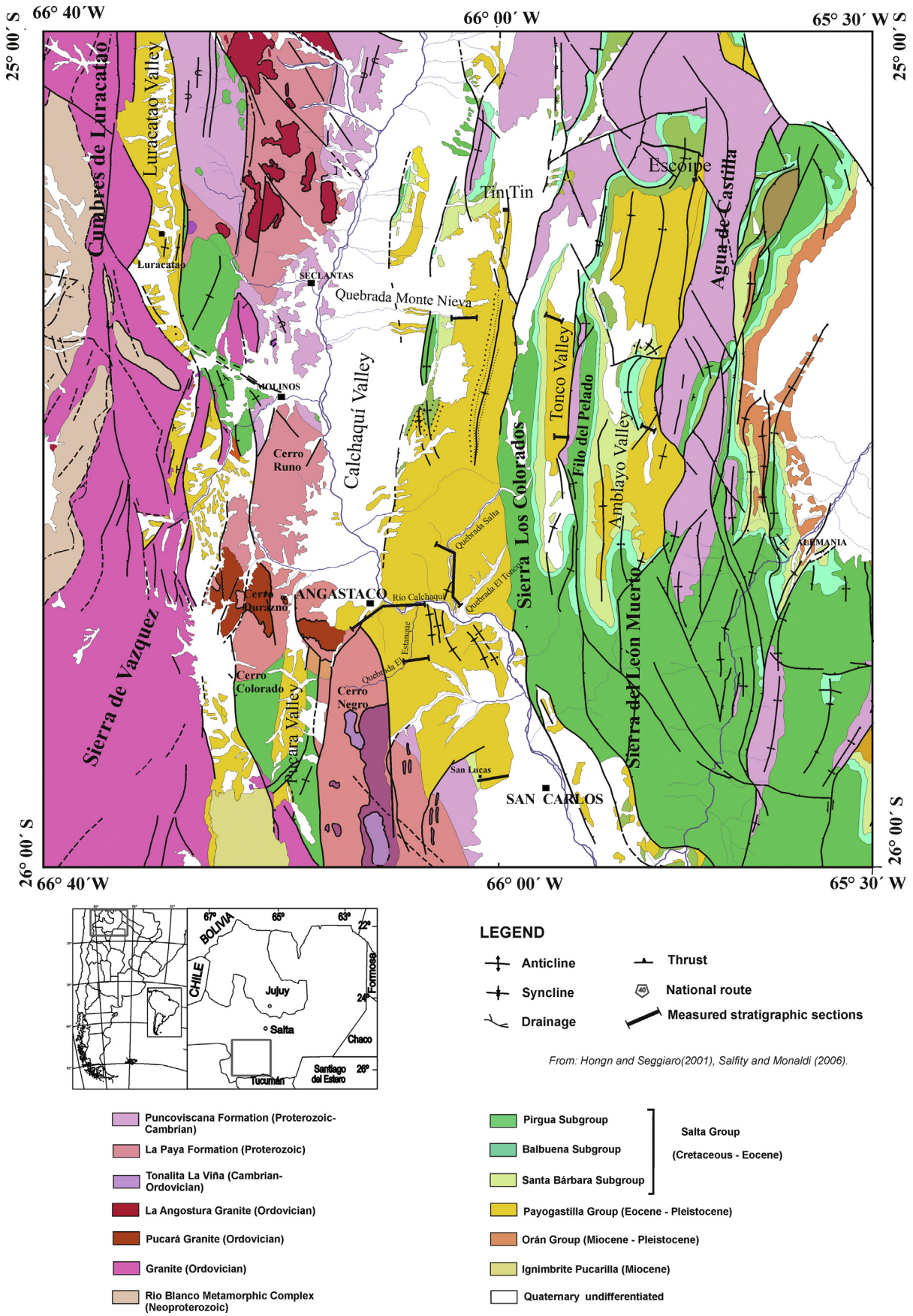

Fig. 1. Geologic map of the Calchaquí, Tonco, and Amblayo regions in southern Salta province, northwest Argentina. Adapted from Hongn and Seggiaro (2001) and Salfity and Monaldi (2006).

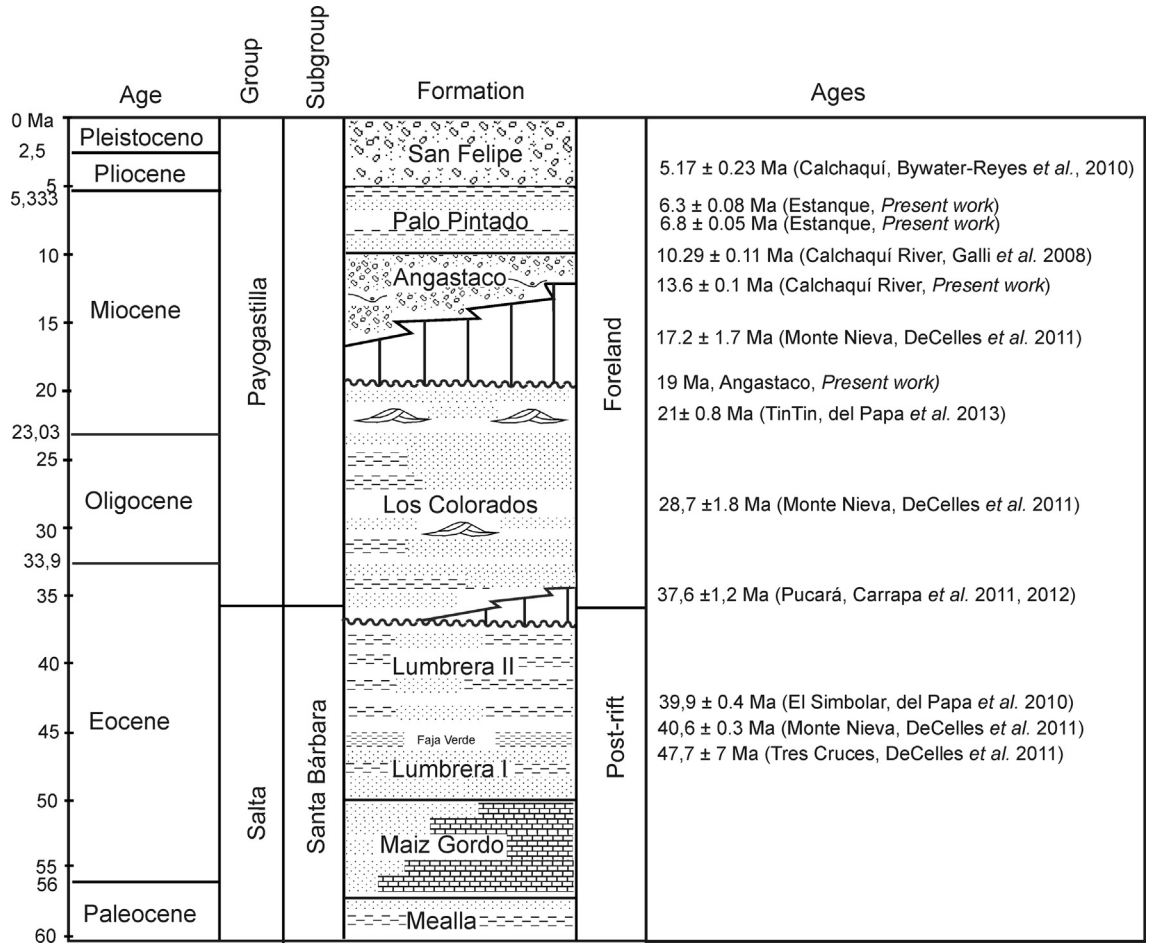

Fig. 2. Lithostratigraphic column of the Cenozoic units from the Calchaquí, Tonco, and Amblayo valley area.

Payogastilla Group began in a sag basin infilled with three sub-basins (Brealito, Pucará and Alemania) that was subsequently inverted by the effects of the subduction of the Nazca Plate and the South American Plate during the Eocene times (Hongn and Seggiaro, 2001). Hongn et al. (2007, 2010 a and b) postulated that the updated record of Eocene deposits in northwestern Argentina indicates a broken foreland basin system in which basement blocks compartmentalized the basin in its initial stages, and a strongly heterogeneous basin basement enhanced the development of this complex broken foreland via the reactivation of Paleozoic and Cretaceous structures. DeCelles et al. (2011) defined a system foreland basin system that began in the Santa Bárbara Subgroup (Salta Group).

In the Calchaquí, Tonco, and Amblayo Valleys, the Payogastilla Group contains a complete stratigraphic record that clearly exposes the relationships with the basement rocks (Figs. 1 and 2).

Despite numerous previous investigations, the stratigraphic divisions of the Payogastilla Group, the evolution of the basin, and the type of basin remain in dispute. In a recent study using detrital apatite fission-track thermochronology, Coutand et al. (2006) concluded that the Cumbre de Luracatao was a topographic high from the lower Miocene (20–18 Ma) until to the Pliocene. During this time, the Puna was disconnected from the Cenozoic foreland basin (Alonso et al., 1991; Vandervoort et al., 1995; Strecker et al., 2007).

DeCelles et al. (2011) interpreted the stratigraphic record of the Cenozoic deposits in northwestern Argentina as a foreland basin system based on the Paleogene clastic lithofacies of the Santa Bárbara Subgroup (Salta Group). They also concluded that the foreland basin evolved because a hypermature area of paleosols ("supersol") developed in different levels of the Mealla, Maíz Gordo, and Lumbrera Formations to the west of the basin. The "supersol" continues to the east as a large unconformity that separates the upper Paleogene and Neogene strata.

Carrapa et al. (2011, 2012) considered the Payogastilla Group to be consistent with a continuous foreland basin system that migrated throughout the area from the upper Eocene to the middle Miocene. U–Pb data from detrital zircon in strata from the Eocene to the Pliocene of the Pucará, Angastaco, and La Viña (Lerma Valley) basins provide a maximum depositional age of 37.6 ± 1.2 Ma for the Los Colorados strata in the Pucará area. del Papa et al. (2013) studied the Payogastilla Group deposits on the western edge of the basin and concluded that the areas that now make up the western and eastern Puna plateau margins were contracted from the middle Eocene to the early Oligocene with the exhumation of the Oire Eruptive Complex (Luracatao Range) (Deeken et al., 2006; Payrola Bosio et al., 2009). Based on a 21 Ma tuff from the basal part of the aeolian deposits, these authors estimated a late early Oligocene age for the isolation of the basins on the Puna plateau.

The Cenozoic Andean foreland basin offers an excellent opportunity to define the relation between tectonism and sedimentation because its history is closely tied to the tectonic control over the evolution of the fluvial system in the Payogastilla basin. In the present contribution, we present the paleoenvironmental

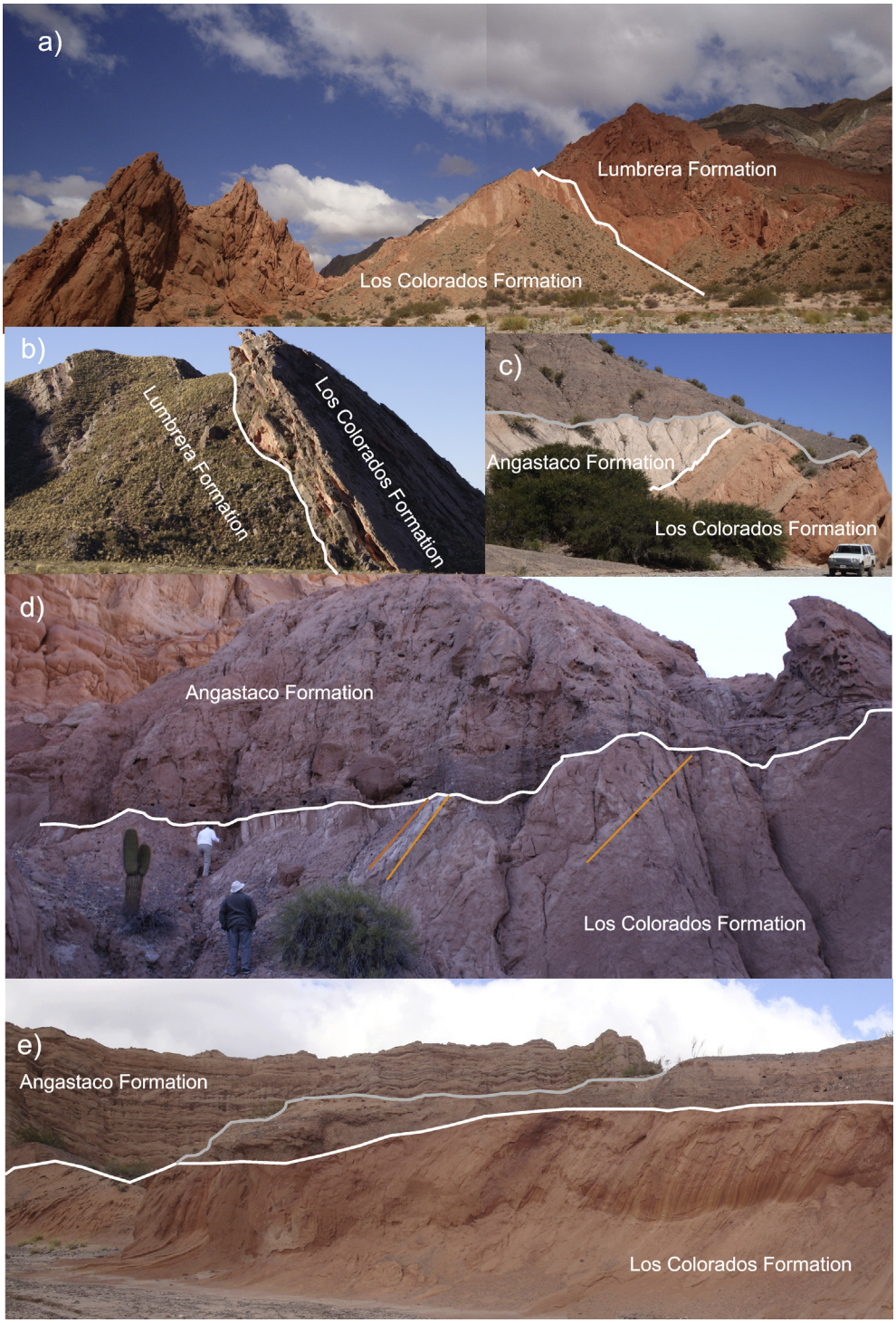

Fig. 3. Characteristics of the contacts between the Lumbrera – Los Colorados and Los Colorados – Angastaco Formations. Contact between the Lumbrera and Los Colorados Formations: a) in Tonco Valley (view to the south) and b) in Amblayo Valley (view to the north). Unconformity contact between the Los Colorados and Angastaco Formations in the Tonco Valley: c) view to the south, d) in view to the north, and e) view to the south.

characteristics, types of unit contacts, depositional origins, paleomagnetic data, and U–Pb provenance ages of the stratigraphic units of the Payogastilla Group. We also present analyses of the basal beds of the Payogastilla Group based on sequence stratigraphy, the differences between the postrift deposits of the Salta Group and the Lumbrera Formation, and the onset of foreland basin development in the Los Colorados Formation deposits. These data clarify the tectono-sedimentary evolution of the basin during the Andean orogeny.

2. Geological setting

The study area is located in the Eastern Cordillera, from 25°42′55″ S to 66°10′44″ W and 25°40′42″ S to 66°05′30″ W,

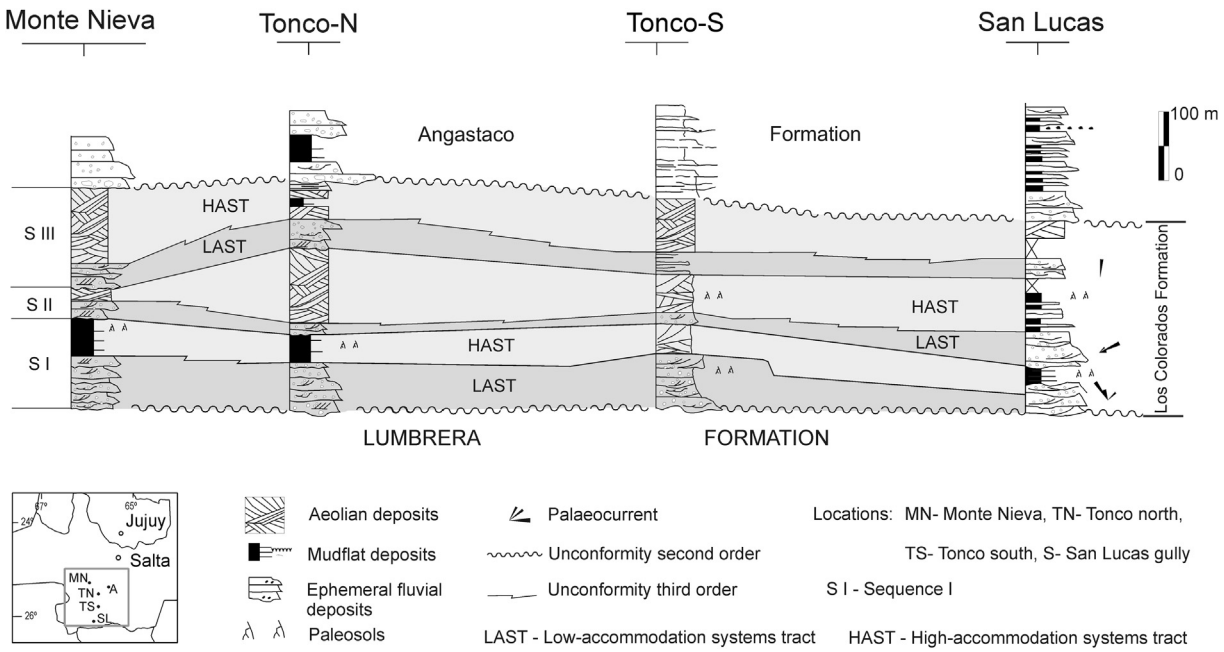

Fig. 4. Correlation of the Los Colorados Formation based on the sequence stratigraphy analysis.

approximately 200 km south of the city of Salta in northwestern Argentina (Fig. 1). Cenozoic sedimentary strata outcrop in the Calchaquí, Tonco, and Amblayo valleys as part of the regional Andean foreland basin that extended into the Eastern Cordillera. In this area, the Upper Neoproterozoic La Paya Formation basement unit contains low-grade metamorphosed sandstones and mudstones (Turner, 1960; Toselli, 1990; Turner and Mon, 1979) that grade southward into schists, gneisses, and migmatites (Aceñolaza and Toselli, 1976; Toselli et al., 1999) in the Sierra de Quilmes and Cumbres Calchaquíes.

The Paleozoic basement is intruded by Cambrian to Ordovician granites (Lork et al., 1990; Lork and Bahlburg, 1993; Omarini et al., 1999) and contains intrusive rocks such as tonalities and pegmatites (La Viña Tonalite, Cambrian), gray granites and pegmatites (La Angostura Granite, Alto del Cajón Granite, Ordovician), and pink granites (Pucará Granite, Alto del Cajón Granite, Ordovician). In the western part of the study area, at the limit of the Eastern Cordillera-Puna, the Sierra de Vázquez (Fig. 1) contains sillimanite schist and migmatite (Metamorphic Río Blanco Complex; Hongn and Seggiaro, 2001). In the north, the Cumbres de Luracatao (Fig. 1) are composed of Paleozoic granites from the eastern border of the Puna (Oire Eruptive Complex), which is a composite unit dominated by porphyritic granites, granodiorite-gabbros and leucogranites that are often mylonitized and metamorphosed (Hongn and Seggiaro, 2001).

A sedimentary succession that overlaps the Neoproterozoic to lower Paleozoic basement corresponds to the Cretaceous-Paleogene strata of the Salta Group (Brackebusch, 1883; *nom. subst.* Turner, 1959) and the Paleogene-Neogene record of the Payogastilla Group.

The Salta Group deposits are divided into the following three subgroups (from base to top): Pirgua (Reyes and Salfity, 1973), Balbuena, and Santa Bárbara (Moreno, 1970). The Pirgua Subgroup is composed of sandstones, conglomerates and siltstones at almost all localities and represents the synrift stage fill. The Balbuena and Santa Bárbara subgroups represent the early and late postrift stage fill, respectively (Salfity and Marquilas, 1994; Marquillas et al., 2005). The Balbuena Subgroup, which accumulated during the Maastrichtian to Early Paleocene, represents the early postrift stage and is formed of white sandstones (Lecho Formation), and the upper part contains gray limestones (Yacoraite Formation). The Santa Bárbara Subgroup consists of the Mealla, Maíz Gordo and Lumbrera Formations (Moreno, 1970) and is dominated by red fine-grained sandstone and siltstone and green mudstone.

In addition, two sub-basins, the Pucará sub-basin (to the south; Hongn and Seggiaro, 2001) and the Brealito sub-basin (to the north; Sabino, 2004) were recognized in the western part of the study area; these sub-basins are part of the Alemania basin (Reyes, 1972) in the central Calchaquí Valley. The Brealito and Luracatao sub-basins (Payrola Bosio et al., 2010) contain outcrops of strata from the Pirgua and Santa Bárbara Subgroups. The Pucará sub-basin only contains outcrops of the Pirgua Subgroup; in the northern Calchaquí Valley (Tin Tin), Tonco, and Amblayo, the entire Salta Group is observed, whereas to the south (San Lucas), only the top of the Santa Bárbara Subgroup is exposed.

The Lumbrera Formation (Moreno, 1970), which represents the uppermost part of the Salta Group (Fig. 2) is composed of claystones and siltstones, and is always reddish-brown to red. Gómez Gomez Omil et al. (1989) identified three units in the Lumbrera Formation based on the contrasting characteristics of the facies groups: the lower Lumbrera Member, the *Faja Verde*, and the upper Lumbrera Member. The lower part is very fossil-rich (Pascual et al., 1981; Bond and Lopez, 1993; Gasparini et al., 1993; Babot et al., 2002) and was dated as lower-middle Eocene based on vertebrate associations (Pascual, 1980).

Based on this subdivision, Starck and Vergani (1996) and del Papa (2006) proposed dividing the Lumbrera Formation into the Lumbrera I (or lower, up to the top of the *Faja Verde*) and the Lumbrera II (or upper), which are separated by an unconformity represented by paleosols and crusting surfaces. Starck and Vergani (1996) considered the foreland basin deposits to begin with Megasequence I, which includes the Lumbrera II and the base of the Los Colorados Formation (Payogastilla Group). del Papa (2006) and del Papa et al. (2010) described the top of the *Faja Verde* as an omission surface that marks the beginning of the sedimentary foreland basin; they stated that the Lumbrera II is equivalent to the basal

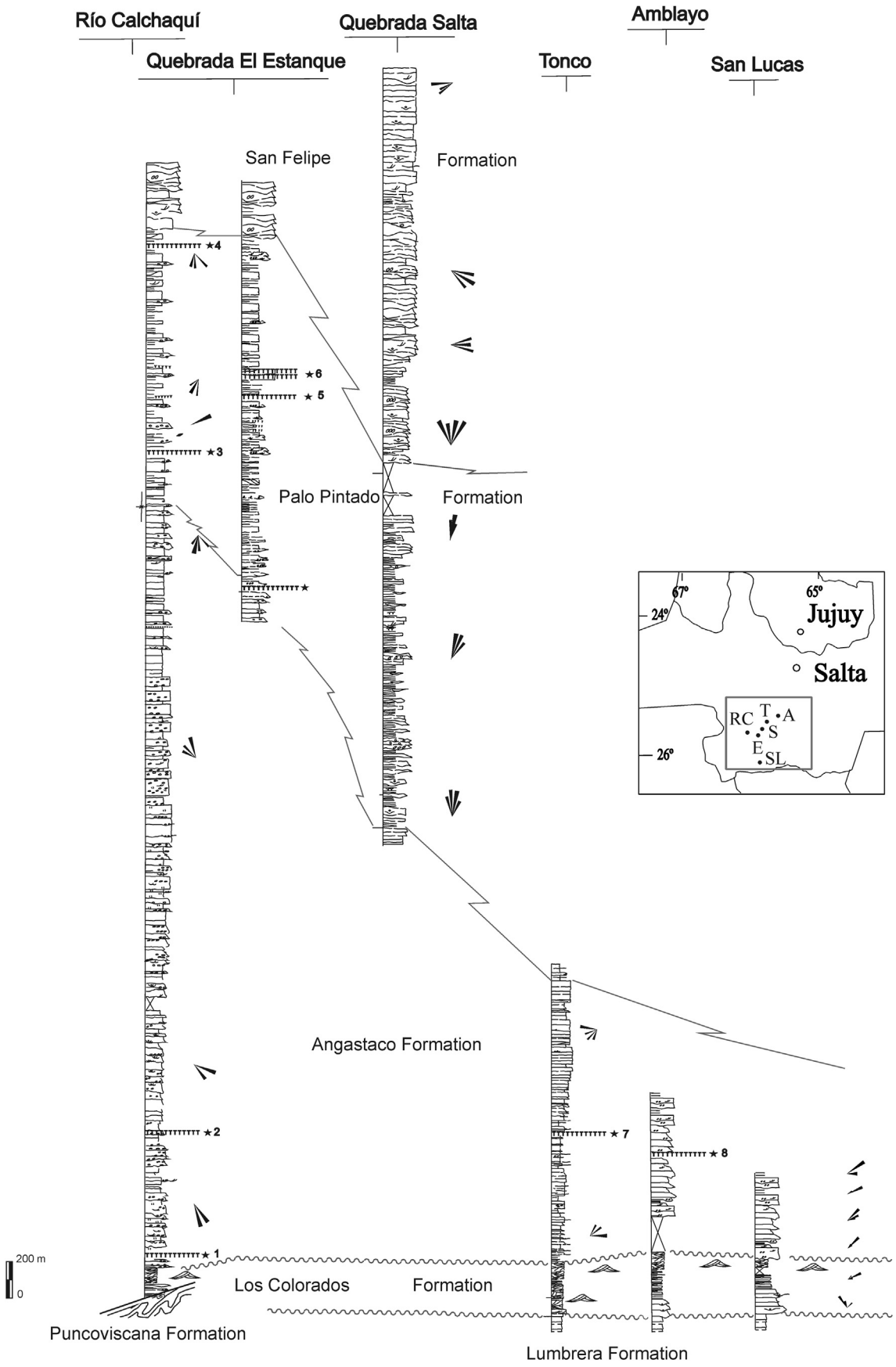

Fig. 5. Stratigraphic correlation of the deposits of the Payogastilla Group.

Table 1
Major lithofacies identified in the Payogastilla Group (modified from Galli and Reynolds, 2012).

Code	Lithofacies	Interpretation
Gmm	Massive conglomerate, poorly sorted matrix-supported clasts, sandy matrix. Strata with abrupt lateral terminations.	Debris flow (high strength). Flows passively occupy pre-existing alluvial topography and mold to the pre-existing channel.
Gmg	Massive conglomerate, matrix-supported clasts with normal grading.	Pseudoplastic debris flow (low strength).
Gcm	Clast-supported, massive conglomerate, with poorly sorted, very angular clasts.	Pseudoplastic debris flow (inertial bedload).
Gh	Clast-supported conglomerate, crudely bedded, sandy matrix. Imbrication.	Longitudinal bars, lag deposits.
Gi	Conglomerate with well-sorted and rounded clasts, sparse matrix, imbrication.	Longitudinal bars.
Gt	Matrix-supported conglomerate with trough cross-bedding.	Minor channel fills.
Se	Sandstone with cosets of grouped trough cross-beds (10– to 20 m thick), very well-sorted, rounded grains.	Aeolian dune deposits.
St	Very coarse sandstone, sets of trough cross-beds. Wedge-shaped strata with residual lag.	Linguoid (3-D) dunes.
Sp	Very coarse sandstone, sets of planar cross-beds and lag deposits. Beds with erosional bases.	Transverse and linguoid bedforms (2-D dunes).
Sl	Fine to coarse sandstone, planar lamination, lag deposits. Tabular beds.	High flow conditions. Flash flood.
Sm	Fine to coarse sandstone, poorly sorted, massive, with clastic wedges and beds with erosional bases.	Upper flow regime and poorly sorted deposits.
Fl	Very fine sandstone, siltstone and mudstone, fine lamination, desiccation cracks, roots, bioturbation.	Overbank, abandoned channel or waning flood deposits.
Fm	Massive siltstone and mudstone, very thin beds.	Overbank or abandoned channel deposits.
Fo	Siltstone and mudstone, very small ripples and very thin laminations.	Swamp and lacustrine in the floodplain.
Po	Very fine sandstone, siltstone and mudstone, massive with calcified rhizoliths penetrating down into sandstone of aeolian dune origin.	Paleosols. The rhizoliths emanate from the bases of damp and wet interdune units.

deposits of the Los Colorados Formation and reported an age of 39.9 ± 0.4 Ma (U–Pb; del Papa et al., 2010) for the Lumbrera Formation. DeCelles et al. (2011) reported an age of 47.7 ± 7 Ma (U–Pb, Paleocene-Eocene) based on data from carbonate-nodule-bearing paleosols (in the Lumbrera *Faja Verde*) in the Tres Cruces area. Detrital zircons from the Lumbrera Formation II in the Quebrada Monte Nieva (Calchaquí Valley) give an age of 40.6 ± 0.3 Ma (middle Eocene, DeCelles et al., 2011). The isotopic age data reported by these authors indicate that the Lumbrera Formation was deposited between 48 and 36 Ma.

Because Starck and Vergani (1996), DeCelles et al. (2011), and Carrapa et al. (2012) reported that the aeolian facies are included in the base of the Angastaco Formation, these facies are assigned a maximum deposition age of 22 to 18 Ma based on fission-track dating (upper Oligocene-lower Miocene; DeCelles et al., 2011). In this present study, based on the analysis of fluvial paleoenvironment and stratigraphic relationships, we included the widely distributed aeolian deposits exposed in the Tonco, Amblayo, and Calchaqui Valleys in the Los Colorados Formation (Fig. 4).

In the Luracatao Valley, the Los Colorados Formation is clearly exposed in the northern part of La Puerta, where it is ~455 m thick and lacks aeolian deposits (Payrola Bosio et al., 2010). This unit unconformably overlies the Lumbrera Formation or lies directly on the Maíz Gordo Formation and exhibits erosional events prior to its deposition.

The deposition of the Los Colorados Formation started in the middle-upper Eocene (del Papa et al., 2004; Payrola Bosio et al., 2009). Detrital zircons from the town of Angastaco have been dated at 37.6 ± 1.2 Ma (Carrapa et al., 2012), and the apatites from Monte Nieva have been dated at 28.7 ± 1.9 Ma (DeCelles et al., 2011). This deposit is ~300 m thick and contains basal sandstone and siltstone facies of an ephemeral fluvial system that are associated with aeolian deposits (Galli and Reynolds, 2012). A tuff horizon intercalated in the aeolian deposits in the Tin Tin section provided an age of 21.0 ± 0.8 Ma (U–Pb; del Papa et al., 2013).

The transition between the Los Colorados Formation and the overlying Angastaco Formation is a paraconformity (Figs. 3–5) and an unconformity (Fig. 3 c and d). The Angastaco Formation (4450-1500 m thick) consists of conglomerates and conglomeratic sandstones in thickening and coarsening-upward cycles with a few siltstone banks at the top of the unit (Fig. 5). Paleoenvironmentally, these deposits are described as a gravel-braided fluvial system (Galli and Reynolds, 2012). Three levels of tuffs are recorded, two of which have been dated: the pyroclastic base dates to 15.26 ± 0.23 Ma (U–Pb; Pereyra et al., 2008), and the tuff in the middle section dates to 13.4 ± 0.4 Ma ($^{40}Ar/^{39}Ar$, section Corte El Cañón; Grier, 1990; Grier and Dallmeyer, 1990). The transition between the Angastaco Formation and the overlying Palo Pintado Formation is sharp and concordant.

The Palo Pintado Formation is ~800 m thick and contains a tuff level that has been dated at 10.29 ± 0.11 Ma (K/Ar) by Galli et al. (2008). Near the top is another pyroclastic level that was dated at 5.27 ± 0.28 Ma ($^{206}Pb/^{238}U$) by Coutand et al. (2006) and at 5.98 ± 0.32 Ma by Bywater Reyes et al. (2010). The unit comprises thickening and coarsening-upward cycles, including matrix-supported conglomerates, fine to medium sandstone, and fine-grained sublithic sandstones that end in levels of green, brown and gray siltstones. These deposits consist of a transitional style between low- and high-sinuosity rivers that form wandering sand-gravel fluvial systems with small lakes (Galli et al., 2011-a; Galli and Reynolds, 2012).

The deposits of the San Felipe Formation at the top of the Payogastilla Group are more than 600 m thick in the southeastern Calchaquí Valley and are affected by numerous faults and folds. The transition between the Palo Pintado Formation and the San Felipe Formation is sharp and unconformable; it contains considerable clast-supported conglomerates with overlapping clasts and a lower proportion of sandstones and siltstones, which are interpreted as a gravel-braided fluvial system (Galli and Reynolds, 2012).

3. Materials and methods

3.1. Sedimentological profiles

Seven sedimentological profiles from the following locations of the Payogastilla Group in the study area were analyzed at a scale of 1:500: 1) along the Calchaquí River (from Quebrada Los Colorados to Quebrada Piedras Blancas), 2) Quebrada El Estaque, 3) Quebrada Salta, 4) Quebrada Monte Nieva, 5) north and south Tonco, 6) Amblayo-Isonza, and 7) San Lucas (Figs. 4 and 5).

The sequence stratigraphy of the Los Colorados Formation was analyzed by considering four well-exposed columns (Fig. 4).

Table 2
Codes for the major architectural elements defined for the Payogastilla Group with their characteristic lithofacies (modified from Galli and Reynolds, 2012).

Formation	Code	Architectural elements	Principal lithofacies
San	GB	Gravel bars	Gmg – Gi – Gt – Sm
Felipe	SB	Sandy bedforms	St – Sm – Fm
	GB	Gravel bars and bedforms	Gt – Gm
Palo	LA	Lateral-accretion macroform	Gt – Sm
	CS	Crevasse splay – Channel	Sp – Sl – Sm
Pintado	FF (CH)	Abandoned channel fills	Fl–Fm
	FF	Foodplain deposits	Fl–Fm – Fo – Po
	SB	Sandy bedforms	Sl – Sm – Fl –
	GB	Gravel bars and bedforms	Gh – Sm –
	DA	Downstream – accretion macroform	Gh – Gi – Gm – Sl – Sm – St
	SB	Sandy bedforms	Sm – St – Sp – Sm
Angastaco	GB	Gravel bars and bedforms	Gh – Gcm
	SG	Sediment gravity flows	Gmg
			Gh – St
	GB	Gravel bars and bedforms	Gh – Gi – Sm
			Gh – Gt – Gmg
			Gh – Gt – Sl
	SB	Sandy bedforms	Sl – St – Sp – Fl – Fm
Los Colorados	LS	Laminated sand sheets associated with aeolian deposits	Sl – Fm – Fl – Se
	SB	Sandy bedforms	Gcm – Sm – St – Sp
	GB	Gravel bars and bedforms	Gm – Gt

Ephemeral fluvial deposits with aeolian dune fields were examined using the concepts of Catuneanu and Elango (2001), Ramaekers and Catuneanu (2004), and, for the non-marine deposits, Catuneanu (2006), Catuneanu et al. (2009).

This research is based on outcrop logging and facies analysis along the Calchaquí, Tonco, and Amblayo Valleys over the past several years. Several characteristics were studied in relatively undisturbed stratigraphic successions, such as lithological types, primary sedimentary structures, discontinuity features and hierarchy, and paleocurrent data.

In the vertical and lateral associations, we examined the geometry and hierarchical organization of the element limits and the variations in the paleocurrents. Sedimentary lithofacies were defined, and the various architectural elements were analyzed (Miall, 2006). The paleocurrent analysis was based on imbricate clasts, cross-bedding, and asymmetrical ripple marks.

To identify different source areas and to relate possible section changes to provenance reorganization through time (e.g. Ingersoll et al., 1984), provenance analyses were carried out on both sandstones and conglomerates, including 30 samples from the Los Colorados Formation, 45 from the Angastaco Formation, 25 from the Palo Pintado Formation, and 10 from the San Felipe Formation.

For the modal sandstone determinations, we used the Gazzi-Dickinson method. At least 300 framework grains were counted per thin section. For the modal counting, the grain types were classified, and detrital modes were counted as the sum of Qm F Lt and Qt F L (Dickinson, 1985).

Conglomerate compositions were analyzed by counting at least 300 clasts per station. The following conglomerate clasts were differentiated: slates, phyllites, schists, gneisses, migmatites, quartzites, quartz, granites, pegmatites, volcanics (paleo and neo), sandstones (gray and red), and limestone (Table 5). Three examples from each formation are plotted showing significant changes.

3.2. U–Pb dating

To improve the stratigraphic correlations in the study area, seven samples (five distal volcanic airfall deposits and two sedimentary deposits) were collected for the U–Pb dating of zircons (Figs. 6 and 7, Table 3). The analyses were carried out by LA-MC-ICPMS at the Laboratory of Geochronology of the Brasilia University (details are presented in the supplementary data, Tables 3 and 4).

3.3. Magnetostratigraphy

The sampling was performed while measuring the stratigraphic separation of the sample sites (~30 m). A minimum of three oriented samples were collected from each site. The ~30 m separation proved to be too wide in parts of the Global Magnetic Polarity Time Scale (GMPTS; Cande and Kent, 1995) that contain short polarity intervals. Subsequent sampling programs attempted to fill in the gaps in the first program.

A total of 22 reversals were found, which define 23 polarity zones. A reversal test of the Class I data (Fig. 12a) demonstrates that the data fall into two distinct antipodal fields, which suggests that the magnetic component isolated by the demagnetization treatments represents the detrital remnant magnetization and not a chemical or thermal postdepositional overprint. The wide scatter in both hemispheres is most likely an artifact of the incomplete demagnetization of the first samples. The mean normal and reversed directions are within 2° (γ_c) of antipodal, which represents a positive reversal test (Class A; McFadden and McElhinny, 1990).

4. Lithofacies, architectural elements, and interpretation of the Payogastilla Group fluvial systems

Fifteen lithofacies and eight architectural elements were recognized in the Payogastilla Group. The lithofacies are presented using the codes of Miall (2006), and are described in Table 1. Table 2 presents architectural elements recognized in each formation.

4.1. Lithofacies, architectural elements, and depositional sequence at Los Colorados

The Los Colorados Formation deposits were correlated using the criteria described in the methodology (Fig. 4). The Los Colorado Formation itself is an unconformity bounded depositional sequence that corresponds to a major stratigraphic cycle in the evolution of the foreland basin in the Calchaquí Valley. The entire package of the Payogastilla Group deposits corresponds to a first-order sequence, i.e., it is associated with one distinct tectonic setting. Hence, according to the hierarchy system based on the magnitude of base-level changes that resulted in the formation of the sequence (Embry, 1995), the Los Colorados Formation can be assigned a second-order level of stratigraphic cyclicity. In this context, the three depositional sequences that form its stratigraphic subdivisions may be regarded as third-order sequences. The correlations reveal that the deposits are separated at the base and top by second-order subaerial unconformities. At the lower boundary of the Los Colorados Formation, the grain size increases, a paleoenvironmental change occurs from the clay playa deposits of the Lumbrera II Formation to ephemeral fluvial systems with conglomerates, and the origin of the sediment changes substantially. This unconformity is very clear in the northern part of Amblayo Valley (Fig. 3 a and b). The controversial upper boundary is an erosional unconformity (Tonco Valley) and represents a change in depositional environment from distal sandy ephemeral currents,

Table 3
U–Pb geochronological data obtained from pyroclastic deposists from Angastaco and Palo Pintado Formations using MC-LA-ICP-MS (Brasilia University).

Sample									Age (Ma)	
	f(206)%	$^{207}Pb/^{206}Pb$	2s (%)	$^{207}Pb/^{235}U$	2s (%)	$^{206}Pb/^{238}U$	2s (%)	rho	$^{206}Pb/^{238}U$	2s (abs)
Angastaco Fm.										
1 LC-A (Calchaqui River section)										
Z6	0,17	0,04751	2,9	0,0137	3,3	0,00209	1,7	0,51	13,4	0,2
Z4	3,10	0,04989	9,2	0,0144	9,5	0,00209	2,6	0,27	13,5	0,3
Z3	0,66	0,04731	4,2	0,0137	4,5	0,00210	1,7	0,37	13,5	0,2
Z8	0,77	0,04888	5,5	0,0142	5,8	0,00211	1,8	0,31	13,6	0,2
Z12	0,76	0,04786	6,0	0,0140	6,3	0,00212	2,1	0,33	13,6	0,3
Z7	0,28	0,04600	3,3	0,0135	3,9	0,00212	2,2	0,55	13,7	0,3
Z1	0,80	0,04686	4,4	0,0138	4,7	0,00213	1,7	0,37	13,7	0,2
Z2	0,40	0,05896	5,3	0,0174	5,5	0,00214	1,5	0,27	13,8	0,2
Z11	0,16	0,05261	3,1	0,0156	4,2	0,00215	2,8	0,67	13,8	0,4
Sample 1-A (Amblayo section)										
Z1	0,12	0,04864	2,0	0,0140	1,3	0,00209	1,6	0,62	13,5	0,2
Z14	0,31	0,05244	3,4	0,0152	4,1	0,00211	2,4	0,57	13,6	0,3
Z18	0,61	0,05559	10,8	0,0162	11,2	0,00212	2,8	0,25	13,7	0,4
Z7	1,49	0,05665	6,6	0,0166	7,0	0,00213	2,1	0,31	13,7	0,3
Z6	1,02	0,07233	14,9	0,0213	15,1	0,00213	2,5	0,17	13,7	0,4
Z5	0,11	0,04795	1,6	0,0141	1,2	0,00214	1,7	0,73	13,8	0,2
Z8	2,23	0,06686	7,7	0,0198	8,1	0,00214	2,3	0,29	13,8	0,3
Z12	0,26	0,07039	2,6	0,0209	2,8	0,00215	1,1	0,41	13,9	0,2
Z15	0,40	0,05686	3,7	0,0169	4,2	0,00216	2,2	0,51	13,9	0,3
Z3	0,96	0,06117	5,9	0,0184	3,1	0,00218	1,8	0,29	14,0	0,3
Z19	0,34	0,05690	4,2	0,0173	5,0	0,00221	2,7	0,55	14,2	0,4
Z13	1,08	0,06873	7,0	0,0209	7,4	0,00221	2,3	0,32	14,2	0,3
Z16	0,27	0,04668	4,4	0,0145	4,7	0,00226	1,7	0,36	14,5	0,2
Sample 20 (El Tonco Valley)										
Z18	0,13	0,04993	1,5	0,0144	2,2	0,00209	1,6	0,74	13,4	0,2
Z2	0,38	0,04655	5,6	0,0136	6,0	0,00211	2,1	0,35	13,6	0,3
Z17	0,21	0,04758	2,1	0,0139	2,6	0,00212	1,5	0,60	13,6	0,2
Z4	0,21	0,04716	3,5	0,0138	3,8	0,00212	1,4	0,38	13,6	0,2
Z1	0,24	0,04616	3,9	0,0136	4,4	0,00213	1,9	0,44	13,7	0,3
Z23	0,22	0,05168	4,4	0,0152	4,9	0,00214	2,2	0,45	13,8	0,3
Z21	0,14	0,04838	3,2	0,0144	3,5	0,00216	1,3	0,39	13,9	0,2
Z14	0,15	0,05856	3,8	0,0175	4,3	0,00217	1,8	0,43	14,0	0,3
Z7	0,21	0,04709	2,4	0,0144	2,7	0,00221	1,3	0,48	14,2	0,2
Z9	0,07	0,04727	1,9	0,0144	2,7	0,00221	2,0	0,73	14,2	0,3
Z13	0,28	0,04490	2,4	0,0137	2,8	0,00222	1,5	0,54	14,3	0,2
Z12	0,46	0,04783	6,3	0,0146	6,4	0,00222	1,6	0,24	14,3	0,2
Palo Pintado Fm. (Quebrada El Estanque section)										
1-PP										
Z6	1,36	0,05286	13,1	0,0070	13,4	0,00096	2,7	0,20	6,2	0,2
Z9	1,65	0,04827	12,1	0,0064	12,4	0,00097	2,5	0,20	6,2	0,2
Z3	0,57	0,04773	5,4	0,0064	6,1	0,00097	2,9	0,47	6,3	0,2
Z14	0,30	0,04895	5,9	0,0066	6,5	0,00098	2,6	0,40	6,3	0,2
Z7	1,02	0,05131	11,8	0,0069	12,3	0,00098	3,5	0,29	6,3	0,2
Z4	1,04	0,04728	5,5	0,0064	6,1	0,00099	2,6	0,42	6,4	0,2
Z16	1,19	0,05066	20,4	0,0069	20,9	0,00099	4,9	0,23	6,4	0,3
Z14	0,57	0,04893	7,2	0,0067	7,5	0,00100	2,4	0,32	6,4	0,2
Z13	0,73	0,05562	6,2	0,0078	6,6	0,00102	2,2	0,33	6,6	0,1
Z2	0,42	0,04468	6,8	0,0063	7,2	0,00103	2,3	0,31	6,6	0,2
Z5	0,81	0,05007	7,8	0,0072	8,1	0,00104	2,4	0,29	6,7	0,2
2-PP										
Z10	0,90	0,04691	7,5	0,0067	9,0	0,00103	4,9	0,55	6,7	0,3
Z7	0,55	0,04563	7,8	0,0066	8,1	0,00105	1,9	0,24	6,8	0,1
Z5	0,95	0,04687	10,2	0,0068	10,5	0,00105	2,4	0,23	6,8	0,2
Z14	1,46	0,04492	13,3	0,0065	13,6	0,00105	2,6	0,19	6,8	0,2
Z6	0,94	0,04502	7,5	0,0066	7,8	0,00106	1,9	0,25	6,8	0,1
Z13	0,35	0,04593	10,5	0,0067	10,7	0,00106	2,0	0,19	6,8	0,1
Z2	1,20	0,04427	9,2	0,0065	9,4	0,00106	2,1	0,22	6,9	0,1
Z8	0,18	0,04642	6,3	0,0068	7,0	0,00107	3,0	0,44	6,9	0,2

clay playa deposition, or aeolian accumulations to a braided fluvial system (Fig. 3 c, d, and e). The Los Colorados Formation deposits were identified as facies of an ephemeral fluvial system with flashy discharge and were associated with calcic paleosols and dune fields, which are characteristic of arid regions.

Two internal third-order subaerial unconformities are identified and form three lower third-order sequences. Sequences I, II, and III comprise a low-accommodation systems tract (LAST) and a high-accommodation systems tract (HAST).

4.1.1. Sequence I

Sequence I is 80–120 m thick. The basal surface is a second-order unconformity that forms the boundary with the underlying Lumbrera Formation, and the upper limit is a third-order paraconformity (Fig. 4). The LAST includes element GB, which typically forms multistory sheets tens to hundreds of meters thick. Flat or irregular erosion surfaces between mesoforms are common. Steeply dipping channel margins are rarely observed. Element SB is typically intercropped and comprises 10% of even the coarsest

Table 4
U–Pb geochronological data from a sabulite level represented by Payo-3 and an arenite level represented by Payo-2 from the Los Colorados Formation obtained using the MC-ICP-MS (Brasilia University).

Sample	f(206)%	Ratios						Ages						% Conc.	rho
		$^{207}Pb/^{206}Pb$	2σ (%)	$^{207}Pb/^{235}U$	2σ (%)	$^{206}Pb/^{238}U$	2σ (%)	$^{207}Pb/^{206}Pb$	2σ (Ma)	$^{207}Pb/^{235}U$	2σ (Ma)	$^{206}Pb/^{238}U$	2σ (Ma)		
PAYO-2 (top of Los Colorados Fm.)															
Z1	0,02	0,05717	0,9	0,5941	2,1	0,07537	1,9	498,3	19,0	473,5	8,0	468,4	8,7	94,00	0,91
Z2	0,01	0,07387	0,6	1,6754	2,1	0,16449	2,0	1038,0	13,1	999,2	13,3	981,7	18,2	94,57	0,95
Z3	0,03	0,07119	1,2	1,2624	4,1	0,12862	3,9	962,8	23,8	829,0	23,0	780,0	28,6	81,01	0,96
Z4	0,88	0,05992	1,2	0,5949	2,5	0,07201	2,2	600,6	25,9	474,0	9,6	448,2	9,7	74,63	0,88
Z5	0,07	0,06108	1,5	0,8204	2,5	0,09742	2,0	641,9	33,0	608,3	11,6	599,3	11,5	93,35	0,79
Z6	0,03	0,07123	0,9	1,4360	2,7	0,14623	2,6	963,9	17,6	904,1	16,1	879,8	21,0	91,27	0,95
Z7	0,06	0,05587	3,1	0,5626	3,6	0,07304	2,0	447,1	67,8	453,2	13,2	454,4	8,6	101,65	0,54
Z8	0,03	0,05690	1,0	0,5727	2,6	0,07300	2,4	487,6	23,1	459,8	9,7	454,2	10,5	93,16	0,92
Z9	0,05	0,05640	1,1	0,5830	2,2	0,07497	1,9	468,0	24,1	466,4	8,1	466,0	8,4	99,58	0,86
Z10	0,85	0,06439	2,6	0,6853	3,3	0,07719	2,1	754,3	54,0	529,9	13,8	479,3	9,9	63,54	0,64
Z11	0,02	0,05956	1,0	0,7069	2,1	0,08607	1,8	587,8	21,1	542,9	8,8	532,3	9,4	90,56	0,89
Z12_CORE	0,01	0,10473	0,6	2,5465	2,6	0,17634	2,5	1709,6	12,0	1285,4	18,6	1047,0	23,8	61,24	0,97
Z12_RIM	0,03	0,05786	1,0	0,6012	2,3	0,07536	2,1	524,6	21,5	478,0	8,8	468,3	9,5	89,28	0,91
Z13	0,03	0,05640	1,1	0,5603	2,7	0,07206	2,4	468,1	24,4	451,8	9,8	448,5	10,6	95,81	0,91
Z14	0,03	0,06055	1,2	0,8066	1,9	0,09662	1,5	623,2	25,2	600,6	8,8	594,6	8,8	95,40	0,80
Z15	0,66	0,04644	5,3	0,0197	5,5	0,00308	1,6	20,7	121,5	19,8	1,1	19,8	0,3	95,91	0,30
Z16	0,01	0,06192	0,8	0,8451	1,9	0,09898	1,7	671,4	16,2	622,0	8,6	608,5	9,8	90,63	0,91
Z17	0,01	0,11559	0,7	5,1188	1,6	0,32117	1,5	1889,2	12,1	1839,2	13,7	1795,4	23,1	95,04	0,91
Z18	0,24	0,05896	2,4	0,6995	3,0	0,08605	1,8	565,5	52,4	538,5	12,5	532,2	9,1	94,10	0,60
Z19	0,04	0,05604	1,0	0,5878	1,6	0,07608	1,3	454,0	21,7	469,5	6,0	472,7	5,8	104,12	0,79
Z20	0,05	0,05955	1,4	0,7355	2,1	0,08957	1,5	587,4	31,3	559,8	9,1	553,0	8,2	94,14	0,73
Z21	0,03	0,05789	0,9	0,6824	2,9	0,08549	2,7	525,7	20,5	528,2	11,9	528,8	13,9	100,61	0,95
Z22	0,04	0,07314	1,4	1,7280	2,5	0,17135	2,1	1017,8	28,3	1019,0	16,1	1019,6	19,6	100,17	0,83
Z23	0,06	0,05638	1,1	0,5768	1,8	0,07421	1,5	467,4	25,0	462,4	6,9	461,4	6,5	98,74	0,79
Z24	0,02	0,07342	1,5	1,6221	2,2	0,16023	1,6	1025,6	29,9	978,8	13,8	958,1	14,6	93,42	0,74
Z25	0,05	0,05605	1,1	0,5860	3,2	0,07583	3,0	454,4	24,0	468,3	11,9	471,2	13,5	103,71	0,94
Z26	0,00	0,17251	0,7	10,2921	4,5	0,43269	4,4	2582,2	11,4	2461,4	41,3	2317,9	85,9	89,76	0,99
Z27	0,03	0,05590	1,1	0,5658	2,5	0,07340	2,2	448,4	24,9	455,3	9,1	456,6	9,8	101,83	0,89
Z28_CORE	0,06	0,06429	0,8	1,1451	2,6	0,12917	2,4	751,3	16,4	774,9	13,8	783,1	17,9	104,24	0,95
Z28_RIM	0,06	0,05776	1,3	0,5895	4,9	0,07401	4,7	520,8	28,5	470,5	18,4	460,3	20,9	88,38	0,96
Z29	0,05	0,05771	0,8	0,5076	3,0	0,06379	2,9	518,7	18,1	416,8	10,2	398,7	11,1	76,85	0,96
Z30	0,03	0,10615	0,8	2,6489	2,6	0,18098	2,5	1734,4	15,6	1314,3	19,4	1072,3	24,6	61,83	0,95
Z31	0,10	0,05735	1,0	0,5855	2,5	0,07405	2,2	504,8	23,1	468,0	9,2	460,5	9,9	91,21	0,90
Z32	0,08	0,05638	1,3	0,5992	2,6	0,07708	2,3	467,2	28,6	476,7	10,0	478,7	10,5	102,46	0,87
Z33	0,08	0,05596	1,2	0,6077	2,1	0,07875	1,8	451,0	26,3	482,1	8,1	488,7	8,3	108,36	0,83
Z34	0,05	0,05769	0,9	0,7018	2,6	0,08822	2,4	518,2	19,4	539,9	10,8	545,0	12,7	105,18	0,94
Z35	0,04	0,05705	1,1	0,6001	2,8	0,07629	2,6	493,4	23,8	477,3	10,6	473,9	11,8	96,06	0,92
Z36	0,03	0,05725	1,3	0,6035	3,3	0,07645	3,0	501,3	29,5	479,4	12,4	474,9	13,6	94,73	0,91
Z37	0,08	0,05887	3,9	0,7385	4,6	0,09098	2,4	562,2	83,5	561,5	19,6	561,3	12,8	99,84	0,52
Z38	0,05	0,05726	2,0	0,6053	3,5	0,07666	2,9	501,6	43,7	480,6	13,5	476,2	13,4	94,92	0,82
Z39	0,03	0,05815	1,2	0,6053	3,1	0,07550	2,9	535,3	25,7	480,6	12,0	469,2	13,2	87,65	0,93
Z40	0,05	0,05701	1,5	0,6187	3,2	0,07871	2,8	492,0	33,3	489,1	12,4	488,4	13,3	99,27	0,88
Z41	0,04	0,11774	0,9	4,2878	4,3	0,26413	4,3	1922,2	15,9	1691,0	35,8	1511,0	57,3	78,61	0,98
Z42	0,06	0,05800	1,0	0,7219	2,8	0,09027	2,6	529,8	22,8	551,8	11,9	557,1	13,8	105,16	0,93
Z43	0,04	0,05634	1,4	0,6347	3,4	0,08170	3,1	465,9	30,7	499,0	13,2	506,3	14,9	108,67	0,91
Z44	0,07	0,05934	1,6	0,7620	4,3	0,09314	4,0	579,6	34,4	575,2	18,7	574,1	21,7	99,05	0,93
Z45	0,02	0,05960	1,2	0,7310	3,0	0,08896	2,8	589,1	26,7	557,1	13,0	549,4	14,6	93,26	0,91
Z47	0,04	0,06608	1,6	1,0283	5,5	0,11286	5,3	808,9	32,6	718,1	28,2	689,3	34,4	85,22	0,96
Z46	0,04	0,07418	1,2	1,6797	3,6	0,16423	3,4	1046,3	23,6	1000,9	22,8	980,3	30,8	93,69	0,95
Z48	0,25	0,06144	3,2	0,8229	5,1	0,09715	4,0	654,6	68,0	609,7	23,5	597,7	23,0	91,31	0,79
Z49	0,10	0,07593	1,9	1,7174	3,5	0,16404	3,0	1093,3	37,6	1015,1	22,5	979,2	26,8	89,56	0,84
Z50	0,02	0,07269	0,9	1,5290	3,6	0,15256	3,5	1005,4	17,6	942,1	22,1	915,3	29,8	91,04	0,97
Z51	0,07	0,05709	1,7	0,6115	2,4	0,07768	1,8	495,1	36,8	484,5	9,4	482,3	8,3	97,42	0,73
Z52	0,06	0,06374	1,6	0,9392	3,1	0,10687	2,6	733,0	34,9	672,5	15,3	654,5	16,5	89,29	0,85
Z53	0,06	0,05713	1,4	0,5818	2,5	0,07386	2,0	496,5	31,0	465,6	9,2	459,4	9,0	92,52	0,82
Z54	0,04	0,05879	1,3	0,6238	3,4	0,07694	3,2	559,5	28,4	492,2	13,5	477,9	14,7	85,41	0,93
Z55	0,04	0,05765	1,1	0,6442	2,3	0,08104	2,0	516,3	25,0	504,9	9,3	502,4	9,9	97,30	0,87
Z56	0,04	0,05864	1,1	0,6204	2,1	0,07673	1,8	553,7	23,3	490,1	8,2	476,6	8,3	86,07	0,86
Z57	0,03	0,05768	1,0	0,6005	2,2	0,07550	1,9	517,8	22,3	477,6	8,2	469,2	8,6	90,62	0,88
Z58	0,11	0,06208	1,5	0,8363	2,4	0,09771	1,9	676,8	32,7	617,1	11,1	601,0	10,6	88,79	0,77
Z59	0,04	0,05725	1,1	0,5889	2,1	0,07461	1,7	501,1	24,4	470,2	7,7	463,9	7,8	92,56	0,84
Z60	0,06	0,08871	0,7	2,9058	1,8	0,23757	1,7	1397,9	13,0	1383,4	13,8	1374,1	21,0	98,30	0,93
Z61	0,02	0,05671	0,8	0,5850	2,3	0,07482	2,1	480,2	18,3	467,7	8,5	465,1	9,4	96,87	0,93
Z62	0,02	0,05650	0,8	0,6114	1,9	0,07848	1,8	472,2	16,9	484,4	7,4	487,0	8,3	103,13	0,92
Z63	0,02	0,05776	0,9	0,6718	2,3	0,08435	2,1	520,7	19,4	521,8	9,2	522,1	10,4	100,26	0,92
Z64	0,02	0,05622	1,6	0,5819	2,3	0,07507	1,7	461,2	35,1	465,7	8,6	466,6	7,6	101,17	0,73
Z65	0,03	0,05640	0,9	0,5794	1,8	0,07451	1,5	468,1	19,7	464,1	6,6	463,3	6,8	98,98	0,86
Z66	0,02	0,05446	1,6	0,5155	3,6	0,06865	3,2	390,2	36,2	422,2	12,3	428,0	13,2	109,71	0,89
Z67	0,02	0,05674	1,1	0,6096	2,3	0,07793	2,1	481,3	23,5	483,3	8,9	483,8	9,6	100,51	0,89
Z69	0,03	0,05698	1,0	0,6189	2,7	0,07878	2,5	490,8	22,5	489,2	10,6	488,8	11,9	99,61	0,93

(*continued on next page*)

Table 4 (*continued*)

Sample	f(206)%	Ratios						Ages						% Conc.	rho
		$^{207}Pb/^{206}Pb$	2σ (%)	$^{207}Pb/^{235}U$	2σ (%)	$^{206}Pb/^{238}U$	2σ (%)	$^{207}Pb/^{206}Pb$	2σ (Ma)	$^{207}Pb/^{235}U$	2σ (Ma)	$^{206}Pb/^{238}U$	2σ (Ma)		
Z70	0,03	0,05639	0,9	0,5928	1,8	0,07625	1,6	467,6	20,1	472,7	6,9	473,7	7,3	101,30	0,87
Z68	0,02	0,05713	1,2	0,6143	2,3	0,07799	1,9	496,5	27,5	486,3	8,8	484,1	8,9	97,51	0,84
PAYO-3 (bottom of Los Colorados Fm.)															
Z1	0,04	0,05803	1,3	0,6508	2,2	0,08134	1,7	531,1	29,0	509,0	8,6	504,1	8,2	94,92	0,79
Z2	0,08	0,05767	4,2	0,6258	4,8	0,07871	2,3	517,1	89,5	493,5	18,6	488,4	10,9	94,44	0,48
Z3	0,05	0,05711	1,3	0,6817	1,7	0,08658	1,1	495,8	29,0	527,8	7,1	535,3	5,8	107,97	0,65
Z4	0,07	0,05926	2,2	0,7279	2,8	0,08910	1,8	576,5	47,0	555,3	12,0	550,2	9,4	95,44	0,63
Z5	0,02	0,06023	1,3	0,7651	2,1	0,09212	1,7	611,9	27,5	576,9	9,4	568,1	9,3	92,84	0,80
Z6	0,04	0,05657	1,5	0,6501	2,1	0,08335	1,5	474,9	32,3	508,5	8,3	516,1	7,3	108,67	0,71
Z7	0,02	0,05639	0,8	0,6153	1,8	0,07914	1,6	467,7	18,2	486,9	6,8	491,0	7,4	104,98	0,89
Z8	0,02	0,05803	1,2	0,6695	2,1	0,08367	1,8	530,9	25,2	520,4	8,6	518,0	8,8	97,57	0,84
Z9	0,04	0,05687	1,3	0,5999	2,2	0,07650	1,8	486,5	27,8	477,1	8,3	475,2	8,2	97,67	0,81
Z10	0,04	0,05724	1,6	0,6174	2,5	0,07824	1,8	500,7	35,2	488,2	9,5	485,6	8,6	96,97	0,75
Z11	0,03	0,05662	1,1	0,6126	1,7	0,07847	1,3	476,8	23,4	485,2	6,4	487,0	6,0	102,13	0,77
Z12	0,04	0,05636	1,1	0,6060	2,0	0,07799	1,7	466,4	25,3	481,0	7,7	484,1	7,7	103,79	0,82
Z13	0,03	0,05792	1,0	0,7246	3,9	0,09073	3,7	526,9	21,7	553,4	16,5	559,8	20,0	106,26	0,97
Z14	0,07	0,06114	1,1	0,6784	1,9	0,08048	1,6	644,2	23,6	525,8	8,0	499,0	7,7	77,46	0,82
Z15	0,03	0,05849	0,9	0,5880	2,1	0,07292	1,9	548,1	19,8	469,6	8,0	453,7	8,5	82,78	0,91
Z16	0,01	0,09590	0,6	3,5006	1,4	0,26474	1,3	1545,8	10,4	1527,3	10,9	1514,1	17,1	97,95	0,92
Z17	0,04	0,05923	1,8	0,6127	2,5	0,07502	1,8	575,5	40,0	485,2	9,8	466,4	7,9	81,04	0,69
Z18	0,02	0,05717	1,0	0,6013	1,7	0,07628	1,4	498,3	20,8	478,1	6,6	473,9	6,6	95,11	0,84
Z19	0,03	0,05711	0,9	0,6132	1,5	0,07788	1,1	495,7	19,6	485,6	5,6	483,5	5,3	97,52	0,79
Z20	0,01	0,05796	0,8	0,6192	1,4	0,07748	1,1	528,4	18,2	489,4	5,3	481,1	5,1	91,05	0,80
Z21	0,02	0,07277	0,7	1,5165	1,5	0,15114	1,3	1007,5	13,7	937,1	9,0	907,4	11,1	90,06	0,89
Z22	0,08	0,05775	1,4	0,6266	2,4	0,07870	1,9	520,3	30,8	494,0	9,2	488,3	8,8	93,86	0,80
Z23	0,07	0,05794	1,1	0,6226	2,0	0,07794	1,7	527,4	23,4	491,5	7,8	483,8	7,9	91,72	0,84
Z24	0,09	0,05655	1,4	0,6048	2,0	0,07758	1,4	473,9	31,3	480,3	7,6	481,6	6,4	101,64	0,69
Z25	0,02	0,05897	0,9	0,6808	1,8	0,08373	1,6	566,1	18,9	527,2	7,3	518,3	7,8	91,57	0,87
Z26	0,06	0,05722	1,2	0,6174	2,2	0,07825	1,9	500,2	25,8	488,2	8,6	485,7	8,9	97,10	0,85
Z27	0,03	0,05861	0,9	0,6568	1,9	0,08128	1,7	552,6	18,7	512,7	7,6	503,7	8,2	91,16	0,89
Z28	0,02	0,05707	1,0	0,6005	2,5	0,07631	2,3	494,4	20,8	477,6	9,5	474,1	10,6	95,89	0,92
Z29	0,02	0,07698	1,0	1,7976	2,2	0,16935	1,9	1120,8	20,0	1044,6	14,3	1008,6	18,2	89,99	0,89
Z30	0,02	0,05668	1,2	0,6025	2,1	0,07711	1,7	479,0	27,6	478,8	8,0	478,8	7,8	99,97	0,80
Z31	0,05	0,05769	1,3	0,6236	3,3	0,07840	3,0	517,9	27,7	492,1	12,6	486,6	14,1	93,95	0,92
Z32	0,03	0,05737	0,9	0,5951	2,0	0,07524	1,9	505,8	18,6	474,1	7,7	467,6	8,4	92,45	0,91
Z33	0,02	0,05687	1,1	0,5801	1,8	0,07398	1,5	486,7	23,7	464,6	6,8	460,1	6,6	94,54	0,81
Z34	0,04	0,05666	1,9	0,5843	2,3	0,07479	1,2	478,5	42,3	467,2	8,4	464,9	5,2	97,17	0,52
Z35	0,03	0,05673	1,3	0,5943	1,9	0,07597	1,4	481,1	28,0	473,6	7,1	472,0	6,3	98,12	0,74
Z36	0,05	0,05703	1,2	0,5882	1,8	0,07481	1,3	492,6	26,8	469,7	6,7	465,1	5,8	94,41	0,72
Z37	0,08	0,05639	1,5	0,5661	2,1	0,07282	1,5	467,6	32,3	455,5	7,6	453,1	6,4	96,91	0,71
Z38	0,06	0,05637	1,7	0,5854	2,2	0,07532	1,5	467,1	37,1	468,0	8,3	468,1	6,6	100,23	0,65
Z39	0,03	0,05659	1,2	0,5984	1,9	0,07669	1,4	475,5	26,7	476,2	7,1	476,4	6,5	100,19	0,76
Z40	0,00	0,11128	1,2	2,5989	4,6	0,16938	4,5	1820,5	22,0	1300,3	33,9	1008,7	41,7	55,41	0,97
Z41	0,08	0,05633	1,5	0,5690	2,1	0,07325	1,5	465,6	32,3	457,3	7,7	455,7	6,5	97,88	0,71
Z42	0,03	0,05674	1,0	0,6002	2,1	0,07671	1,9	481,6	21,6	477,3	8,2	476,5	8,7	98,93	0,89
Z43	0,03	0,05669	1,1	0,5780	1,9	0,07395	1,6	479,5	24,8	463,2	7,2	459,9	7,0	95,92	0,82
Z44	0,06	0,06348	3,6	0,6232	4,6	0,07119	2,9	724,5	74,9	491,8	17,9	443,3	12,5	61,20	0,63
Z45	0,03	0,05678	0,9	0,5795	2,2	0,07402	2,0	483,0	19,9	464,1	8,2	460,3	8,9	95,30	0,91
Z46	0,02	0,05964	0,7	0,6460	2,6	0,07855	2,5	590,6	16,2	506,0	10,4	487,5	11,7	82,54	0,96
Z47	0,01	0,07425	0,6	1,7538	3,2	0,17130	3,1	1048,4	12,8	1028,6	20,8	1019,3	29,7	97,23	0,98
Z48	0,02	0,05736	1,2	0,5843	3,1	0,07387	2,9	505,6	26,4	467,2	11,7	459,4	12,8	90,88	0,92
Z49	0,00	0,06426	0,9	0,8746	2,5	0,09871	2,3	750,2	19,0	638,0	11,8	606,8	13,4	80,88	0,93
Z50	0,03	0,05571	1,0	0,5890	2,0	0,07669	1,7	440,8	22,5	470,2	7,6	476,3	8,0	108,07	0,86
Z51	0,07	0,05826	1,6	0,7000	2,8	0,08714	2,3	539,6	34,6	538,8	11,7	538,6	11,9	99,81	0,83
Z52	0,02	0,05565	1,1	0,5290	4,8	0,06894	4,7	438,3	23,7	431,1	16,8	429,8	19,4	98,06	0,97
Z53	0,02	0,05748	0,8	0,6795	2,4	0,08575	2,3	509,8	18,4	526,5	9,9	530,3	11,5	104,02	0,94
Z54	0,01	0,06096	0,6	0,9000	1,6	0,10707	1,5	637,9	12,7	651,7	7,9	655,7	9,6	102,78	0,93
Z55	0,02	0,06098	1,1	0,7496	2,1	0,08915	1,8	638,4	23,7	568,0	9,3	550,5	9,7	86,23	0,86
Z56	0,03	0,05603	1,0	0,5952	2,0	0,07704	1,7	453,5	21,5	474,2	7,6	478,5	8,0	105,51	0,87
Z57	0,05	0,05695	1,4	0,5995	2,3	0,07635	1,9	489,7	30,1	476,9	8,8	474,3	8,6	96,86	0,81
Z58	0,04	0,05658	1,1	0,6073	1,8	0,07785	1,4	475,2	24,2	481,9	6,8	483,3	6,5	101,71	0,79
Z59	0,07	0,05640	1,7	0,5904	2,4	0,07592	1,7	468,1	37,4	471,1	9,0	471,7	7,7	100,78	0,71
Z60	0,02	0,05796	1,1	0,6912	2,3	0,08648	2,0	528,3	23,1	533,5	9,4	534,7	10,2	101,21	0,88
Z61	0,01	0,06889	0,8	1,2224	1,7	0,12869	1,5	895,5	15,5	810,9	9,5	780,4	11,2	87,14	0,90
Z62	0,03	0,05658	1,3	0,6047	3,2	0,07752	2,9	475,1	28,8	480,2	12,2	481,3	13,5	101,31	0,91
Z63	0,02	0,06323	1,2	0,7329	2,9	0,08406	2,7	716,0	24,5	558,2	12,5	520,3	13,4	72,67	0,92
Z64	0,03	0,05636	0,8	0,5720	2,2	0,07361	2,0	466,6	18,8	459,3	8,1	457,8	9,0	98,12	0,92
Z65	0,04	0,05702	1,0	0,6004	2,0	0,07637	1,7	492,2	21,7	477,5	7,5	474,4	7,8	96,39	0,87
Z66	0,18	0,06589	2,0	0,7132	2,7	0,07851	1,8	802,7	41,0	546,7	11,2	487,2	8,3	60,70	0,66
Z67	0,02	0,05342	1,2	0,2153	2,4	0,02923	2,1	346,8	27,0	198,0	4,3	185,8	3,8	53,56	0,86
Z68	0,05	0,05952	1,6	0,6673	2,6	0,08131	2,0	586,3	35,7	519,1	10,7	503,9	9,9	85,95	0,78
Z69	0,04	0,05714	1,1	0,6185	2,1	0,07851	1,8	497,1	24,3	488,9	8,1	487,2	8,3	98,02	0,85
Z70	0,15	0,06046	5,1	0,6336	5,6	0,07601	2,2	619,9	107,2	498,3	21,9	472,3	10,3	76,18	0,40

Table 4 (*continued*)

Sample	f(206)%	Ratios						Ages						% Conc.	rho
		$^{207}Pb/^{206}Pb$	2σ (%)	$^{207}Pb/^{235}U$	2σ (%)	$^{206}Pb/^{238}U$	2σ (%)	$^{207}Pb/^{206}Pb$	2σ (Ma)	$^{207}Pb/^{235}U$	2σ (Ma)	$^{206}Pb/^{238}U$	2σ (Ma)		
Z71	0,03	0,05838	1,1	0,6863	2,1	0,08526	1,8	544,0	23,8	530,6	8,6	527,5	9,0	96,96	0,85
Z72	0,07	0,06995	1,4	1,4577	2,7	0,15114	2,3	926,9	29,5	913,0	16,3	907,3	19,3	97,89	0,85
Z73	0,03	0,07563	1,2	1,3169	3,3	0,12629	3,1	1085,3	23,4	853,2	19,1	766,7	22,5	70,64	0,94
Z74	0,01	0,06977	0,8	1,3857	1,9	0,14404	1,7	921,7	16,3	882,8	11,1	867,4	13,8	94,12	0,91
Z75	0,02	0,05746	0,9	0,6159	2,6	0,07774	2,5	509,1	19,0	487,3	10,1	482,6	11,5	94,80	0,94
Z76	0,00	0,05705	0,7	0,5827	2,1	0,07409	2,0	493,4	15,2	466,2	7,8	460,7	8,8	93,38	0,94
Z77	0,03	0,05865	1,2	0,6076	2,3	0,07514	1,9	554,2	26,9	482,1	8,8	467,0	8,7	84,27	0,84
Z78	0,07	0,05642	1,7	0,5808	2,7	0,07467	2,1	468,8	37,7	465,0	10,2	464,2	9,6	99,01	0,78
Z79	0,01	0,07379	0,8	1,4572	2,6	0,14323	2,5	1035,7	15,2	912,9	15,5	862,9	19,8	83,31	0,96
Z80	0,04	0,05673	1,4	0,5762	2,4	0,07367	1,9	480,9	30,4	462,0	8,8	458,2	8,5	95,28	0,81

gravel successions; this represents slack water deposits such as abandoned channel fills and bar-edge sand wedges. These deposits are interstratified with tabular sandstone facies (Facies Sp, and Sm).

Near the top, this sequence changes to the sandy bedform deposits, fine-grained sandstones, and laminated mudstone (element LS) that form unconfined ephemeral deposits and clay playas with paleosol (Tunbridge, 1984). The grain size gradually decreases upwards, which is consistent with the lowering in the energy regime of the fluvial systems. The southern Tonco section contains dune fields (Figs. 4 and 8a) that represent the HAST and are interpreted as a period of tectonic inactivity.

4.1.2. Sequence II

This sequence is 50–100 m thick and is limited by subaerial unconformities (third-order surfaces) at the base and top. The basal facies include a multistory succession of stacked channel fill macroforms. The fluvial features range from confined ephemeral proximal (element SB) at the base (LAST; Fig. 4) to unconfined ephemeral deposits (element LS) composed of moderately sorted and rounded sandstone with a well-developed nodular calcrete paleosol and laminar calcrete horizons (Facies Po) in aeolian deposits at the top (Facies Se, HAST; Figs. 4 and 8 b).

4.1.3. Sequence III

Sequence III is 100–120 m thick and is similar in character to Sequence II. This sequence records a change from confined ephemeral proximal facies (element SB) at the base (LAST, Fig. 4) to aeolian deposits at the top (HAST). The lower bounding surface is the third-order subaerial unconformity, which erodes into sequence II in the southern part of Tonco Valley (Fig. 4 a and 5). The upper sequence boundary is represented by the second-order subaerial unconformity, which is clear in northern and southern Tonco Valley (Fig. 3 d and 4) and marks the sharp limit between the Los Colorados and Angastaco Formations.

The base of the each sequence (I, II and III), represented by amalgamated channel deposits indicates a low accommodation setting, whereas floodplain-dominated successions are interpreted to form under high-accommodation conditions. In these sequences, the fluvial accommodation would have been created by differential tectonic movement between the basin and source area under constant climatic conditions during the deposition of the Los Colorados Formation. The change in the extent of channel amalgamation between low- and high-accommodation systems tracts may be an expression of fluvial sedimentation occurring under varying accommodation conditions.

4.2. Angastaco Formation

Four profiles in the Angastaco Formation were described along the Calchaquí, San Lucas, Tonco southern, and Amblayo Rivers. This formation is 1550–4340 m thick but is > 850 m thick in Amblayo and >520 m thick in San Lucas. Sequential stratigraphic analysis could not be performed in the Angastaco Formation because many portions of the sections are incomplete due to erosion or faulting.

Based on the lithofacies and architectural elements, several fluvial systems were recognized. The lithofacies were characterized according to the codes of Miall (2006), with modifications based on the deposits' properties (Table 1) and the analysis of the architectural elements. Table 2 shows the most important architectural elements and their codes.

Three fluvial systems were defined for the Angastaco Formation: 1) a shallow gravel-bed braided system at the base that transitions into 2) a deep gravel fluvial system at the top and 3) a middle fluvial section on the border of the basin along the Calchaquí River, which is associated with common gravity flow deposits.

4.2.1. Shallow gravel-bed braided fluvial system

Element GB is predominant (Fig. 8c) and consists of tabular sections with numerous internal erosional surfaces that are characterized by tractive current deposits in which Gh, Gi, and Gt form superposed longitudinal bars and minor channel fills (Miall, 1985). To a lesser extent, they include Gmm debris flow facies (high strength) that occupy the pre-existing fluvial topography (Fig. 3d) and Gmg pseudoplastic (low strength) debris flow facies (Table 1). Massive or crudely stratified conglomerates (Gcm) represent channel-floor or core-bar deposits that are followed by large-scale planar tabular sets of cross-bedded conglomerates and sandstone.

Large channels are common; they are 1 m or less deep and may be abandoned or filled with lenticular or wedge-shaped sand beds (Facies Sp, Sl, St, and Sm) that generated elements SB when low flow systems were present (Miall, 1994, 1995, Fig. 8c).

4.2.2. Gravel-braided fluvial system associated with gravity flow deposits

These deposits are typical of distributary fluvial systems that connect with alluvial fan deposits (Miall, 1995).

Element GB is dominant and consists of gravel bars and bedforms. Gravel bars and bed deposits comprise facies Gh, Gt, and Gmm. These deposits have sharp erosional bases and often erode sand bedforms and channels. They are lobate or sheet-like in geometry. The gravel bars and bedforms are usually up to 2 m thick and are rarely up to 4 m thick. The erosional relief of the gravel bars varies between 0.5 m and 2 m. They consist of fine- to coarse-grained conglomerates of the Gh and Gt facies. The coarse-grained conglomerates (Gmm) or channel bedforms (Gh), with a few centimeters thick, within the channel just above the erosional base suggesting that gravel bar erosion and subsequent deposition occurred within the channel. This pattern indicates a sudden increase in the velocity of the depositional current.

Table 5
Conglomerate clast compositions normalized to 100%.

Profile	Formation	Sample	Slate + Phyllite %	Schist %	Gneis + Migmatite %	Quartzite %	Quartz %	Granite %	Pegmatite %	Volcanics CEO %	Sandstone %	Neovolcanics %
		1	45	0	0	3	3	21	10	15	3	0
		2	61	0	0	0	19	10	0	1	4	5
		3	74	0	0	2	6	9	0	2	2	5
		4	70	0	0	0	20	10	0	0	0	0
		5	73	0	0	0	18	9	0	0	0	0
Tonco south	Angastaco	6	62	0	0	0	13	21	0	0	4	0
		7	40	10	0	0	40	10	0	0	0	0
		8	48	0	0	0	19	33	0	0	0	0
		9	52	0	0	0	20	24	0	1	3	0
		10	59	7	0	0	9	20	0	0	2	3
		11	33	11	0	0	11	34	11	0	0	0
		12	40	10	0	0	10	30	5	0	5	0
		13	43	9	0	0	13	31	2	0	0	2
		14	43	11	0	0	9	28	5	2	2	0
		15	44	8	0	0	7	30	5	0	6	0
		16	38	17	0	0	15	30	0	0	0	0
		17	51	12	0	0	5	30	0	0	2	0
		18	43	9	0	0	13	35	0	0	0	0
		1	25	19	0	15	10	19	12	0	0	0
		2	4	0	32	10	6	32	16	0	0	0
	Los	3	2	7	0	11	20	22	35	3	0	0
		3′	5	14	5	2	8	38	28	0	0	0
	Colorados	3″	0	15	5	10	20	31	19	0	0	0
		4	1	10	10	12	20	20	25	2	0	0
		5	0	15	10	10	40	20	5	0	0	0
		6	20	0	15	10	10	35	10	0	0	0
		7	18	15	20	12	10	20	5	0	0	0
		8	0	5	15	11	10	30	29	0	0	0
		9	40	8	5	10	10	24	3	0	0	0
Calchaquí		10	40	10	3	5	15	22	5	0	0	0
		11	27	5	20	5	15	20	5	3	0	0
		12	17	13	12	11	20	22	2	3	0	0
	Angastaco	13	0	17	10	15	20	33	5	0	0	0
		14	33	0	20	7	20	20	0	0	0	0
River		15	50	1	4	2	8	35	0	0	0	0
		16	63	5	0	7	10	10	5	0	0	0
		17	65	8	3	1	2	14	7	0	0	0
		18	1	0	20	5	20	49	5	0	0	0
		19	50	0	8	3	7	25	5	2	0	0
		20	80	0	2	1	1	14	0	2	0	0
		21	90	0	5	1	4	0	0	0	0	0
		22	50	0	0	9	10	21	10	0	0	0
		23	10	0	0	4	11	55	10	0	10	0
	Palo	24	19	17	0	5	15	13	13	0	18	0
	Pintado	25	15	27	0	9	10	19	7	0	13	0
		26	10	20	0	8	10	32	10	0	10	0
Estanque	Palo	1	34	3	3	0	27	18	15	0	0	0
	Pintado	2	39	5	1	0	19	26	10	0	0	0
	Los	1	60	0	0	0	19	10	0	10	0	1
Monte	Colorados	2	72	0	0	0	9	11	0	8	0	0
Nieva	Angastaco	1	9	0	0	0	13	78	0	0	0	0
	Los	1	15	5	5	0	40	30	5	0	0	0
	Colorados	2	8	0	20	0	40	15	17	0	0	0
		3	15	10	0	5	35	30	0	0	0	5
San		4	18	0	13	0	35	26	0	0	0	8
	Angastaco	5	18	0	12	0	34	22	0	0	0	14
Lucas		6	20	0	4	0	29	32	0	0	10	5
		7	15	0	15	4	26	27	0	0	5	8
		8	18	5	8	0	30	20	0	0	10	9
		1	47	0	0	0	12	22	19	0	0	0
Peñas		2	62	0	0	0	14	15	9	0	0	0
	Palo	3	49	0	3	0	17	22	0	0	9	0
Blancas	Pintado	4	59	0	0	0	18	11	0	0	12	0
		5	56	0	0	0	16	15	3	0	10	0
		6	49	0	0	0	23	13	2	0	13	0
		1	63	0	0	0	13	20	4	0	0	0
	Palo	2	59	0	0	0	18	17	6	0	0	0
Quebrada	Pintado	3	54	0	0	0	15	19	4	0	8	0
		4	49	0	0	5	14	19	4	0	9	0
Salta		5	58	0	0	6	9	13	0	0	14	0
	San	6	50	5	0	0	5	20	5	0	15	0
	Felipe	7	45	5	2	0	3	30	5	0	10	0

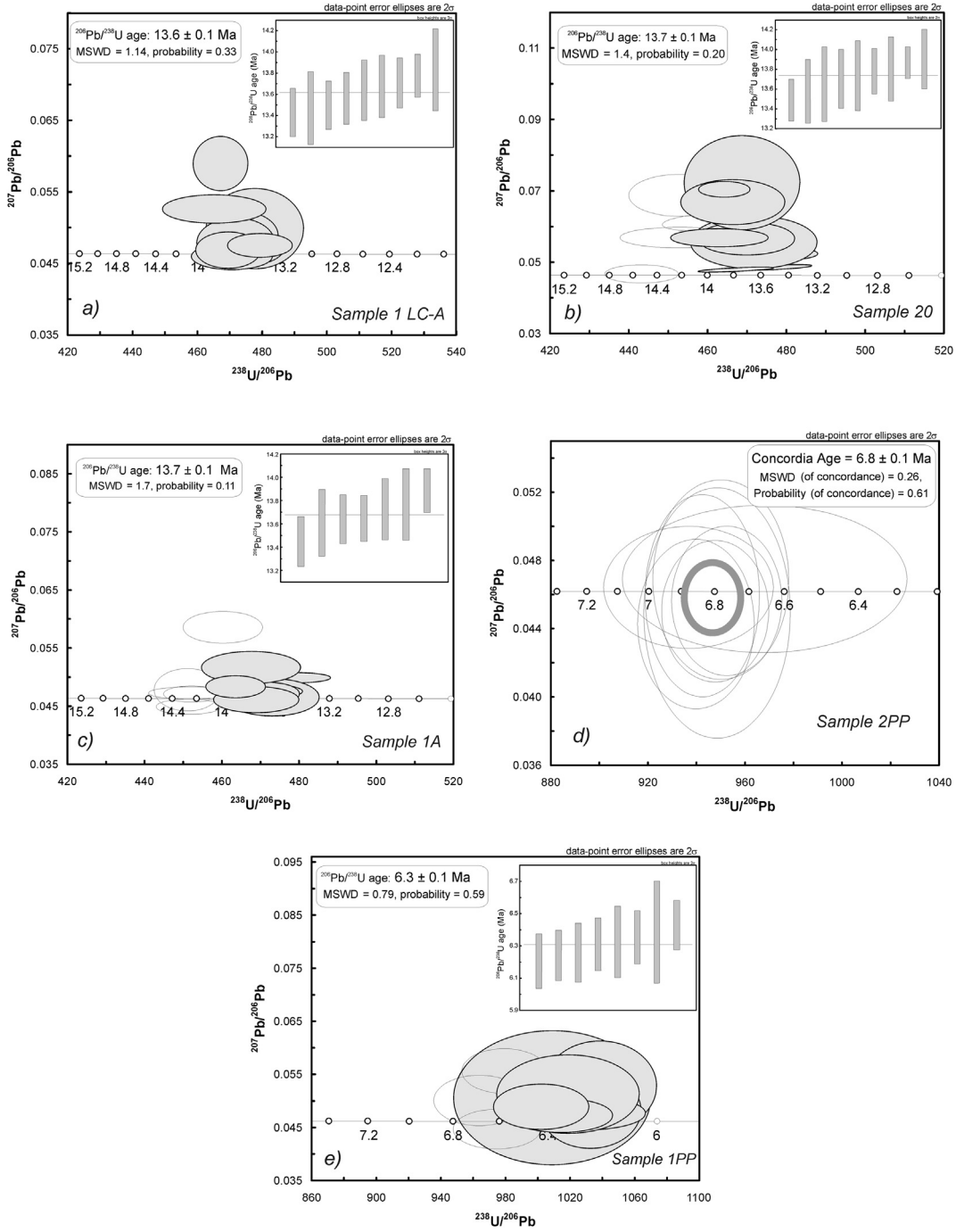

Fig. 6. Tera-Wasserburg concordia plots and weighted mean $^{206}Pb/^{238}U$ ages (insets) for studied samples. Analyses used for the age calculations (a, b, c, d) are shaded. Plots and calculations based on ISOPLOT of Ludwig (2003).

The characteristic deposit types are the SG elements of sedimentary gravity flows, which are related to high-energy flow deposits (Fig. 8c). These deposits consist of matrix-supported massive gravels (Gmm). They have sharp erosional bases and are shaped like elongate lobes. These deposits are underlain by gravel or sand bars, and they also occur within channel deposits, are between 2 m and 4 m thick, and their presence within the channel fills most likely records channel bank instability and slumping.

4.2.3. Deep gravel-braided fluvial system

This system consists of a high proportion of clast- and matrix-supported conglomerates and gravel-sandy and subordinate sandy facies that form elements GB and DA. Element GB dominates at the cycle base; thus, the gravel-sandy bars have macroforms of element DA at the top (Fig. 8d).

This succession includes major and minor channels and bar surfaces. The major channels are limited by fourth-order erosional surfaces with ramps up to 2.5 m thick, whereas the minor channels are separated by third- and second-order surfaces. The channels are filled with facies Gh, which forms dune and gravel lag deposits, and with facies St, Sl, and Sm, which consist of lobulated bars separated by second-order surfaces.

Downstream accretion macroforms (element DA) comprise facies Sl, Sm, St, Gm, Gi and Gh (sand and gravel bedform deposits),

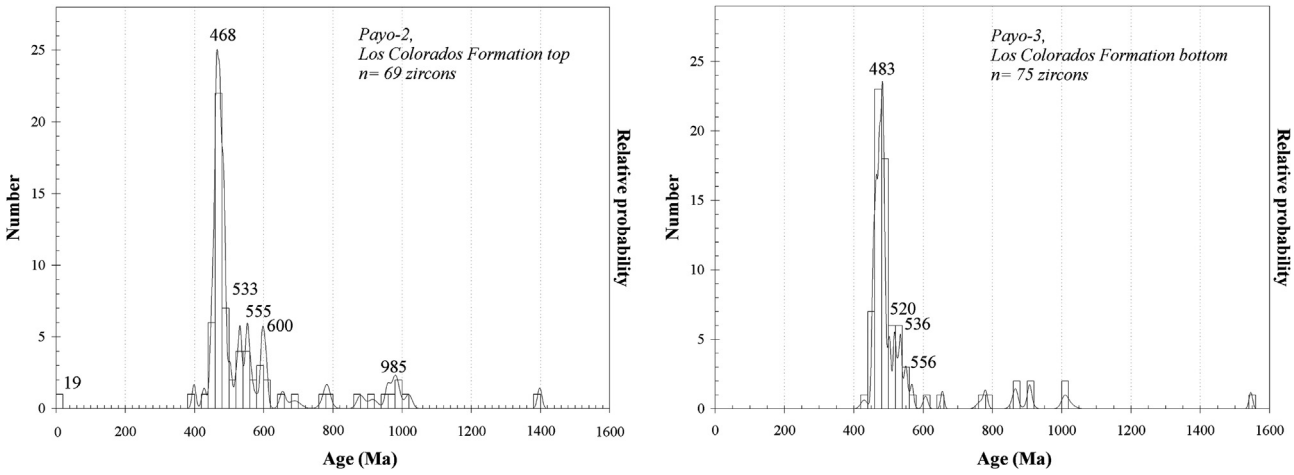

Fig. 7. Probability density plot diagram for samples from the Los Colorados Formation plots and calculations based on ISOPLOT according to Ludwig (2003).

which have sheet-like geometries. Downstream accretion macroforms record channel deposition. The interpretation of the accretion surfaces is based on knowledge of the paleocurrent directions, in cases where the paleocurrent directions are subparallel to the accretion surfaces, they are considered to be downstream accretion.

4.3. Palo Pintado Formation

The fluvial architectural characteristics and associated lithofacies in the Palo Pintado Formation define a fluvial system with intra-channel and overbank deposits (Galli et al., 2011-b). The intra-channel accumulations include gravel bars and bedform deposits (GB) and sandy bedforms comprising transverse bars and sand waves formed by vertical accretion and downstream flow (SB). In contrast, the overbank deposits are represented by three types of features: a) lateral accretion macroforms, which are characterized by large-scale, gently-dipping second-order bounding surfaces that correspond to successive increments of lateral growth, with erosional bases and gradational tops; b) small crevasse splay channels resulting from erosion at the borders of the main channel during flood events, which correspond to crevasse channels (CS); and c) the development of large floodplain deposits (FF).

The Palo Pintado Formation lithofacies are characteristic of an intermediate stage between low-sinuosity, multiple channel rivers (classic braided rivers) and high-sinuosity, single channel rivers (classic meandering rivers; Schumm, 1981, 1985; Miall, 2006).

In some sections, these rivers can develop a simple channel, whereas in others, they develop multiple channels. In contrast to the proposal of Miall (1985), element SB is important in this lithofacies, and it is defined as a “gravel-sandy sinuous fluvial system” (Fig. 8e).

This fluvial system developed large alluvial plains (FF) that were desiccated in the dry season or for longer intervals, as is reflected by desiccation cracks (Fl) and thin sheets of gypsum and pedogenetic characteristics (Fo). The fine to very fine sandy lithofacies that alternate with siltstone and mudstone beds resulted from flooding in these lagoons during heavy rainfall events (Galli et al., 2011-b).

The swamp sub-environment (lithofacies Fm and Fl) is found at borders of lagoons where colmatation processes operated and there was little accommodation space for sedimentation. This environment also represents the final stage in which the lagoon coverings were filled as sediment accumulation reached a maximum in the alluvial plains.

We can infer that stable climate conditions allowed the paleoenvironment and the paleocommunities to persist for a long time (between 10 and 5 Ma) and that a warm, humid, tropical to subtropical climate with a slight seasonality was the norm (Starck and Anzotegui, 2001; Galli et al., 2011-b). This interpretation is substantiated by fossil evidence, including 1) Caiman cf *C. latirostris* (Bona et al., 2011, 2013); 2) common pelecypods; 3) leaf impressions from plants such as *Salvinia* and pteridophytes (*Acrostichum paleoaurum*, Blechnum sp.); 4) angiosperms (Cyperaceae, Lauraceae, Meliaceae, Euphorbiaceae) (Herbst et al., 2000); and 5) clay minerals such as illite, smectite, and kaolinite that are representative of an alluvial plain subenvironment.

4.4. San Felipe Formation

Braided alluvial fans — Shallow gravel-braided fluvial system. The San Felipe Formation is characterized by conglomerate deposits in low-sinuosity channels with considerable GB elements (Fig. 8f). Most of the beds are tabular with many minor internal erosion surfaces and tractive current deposits (Facies Gmg, Gt and Gi; Fig. 8f). Abandoned low-flow channels that are filled with sand lenses form subordinate SB elements. The conglomerate facies tend to be thick (more than 7 m) and contain multi-episodic deposits in gravel-dominated distributary alluvial fan deposits (Miall, 2006). The well-sorted conglomerates lack a matrix, contain rounded clasts that overlap in thick tabular strata that are 2 to more than 7 m thick, and are found in longitudinal bar deposits (Facies Gi). The unit also contains poorly sorted conglomerates, supported clasts, pseudoplastic debris flows (Facies Gmg), and poorly sorted deposits and coarse massive wackes that are the result of rapid accumulation (Facies Sm).

5. Petrographic components

5.1. Petrographic components of the conglomerates

The conglomerate facies of the Payogastilla Group deposits were classified as petromictic orthoconglomerates and, to a lesser extent, paraconglomerates. Clast counting (Fig. 9) reveals the presence of slates, phyllites, and schists from the Puncoviscana Formation; white and pink granites, gneisses, migmatites and pegmatites from the Oire Eruptive Complex; and smaller amounts of paleovolcanic clasts from the Oire Eruptive Complex of the Western Northern Puna (Ordovician). These data are associated with paleocurrent directions from the west, and southwest (Fig. 4).

The Angastaco Formation conglomerates contain substantial amounts of plutonic rocks from the Complejo Eruptivo Oire in the

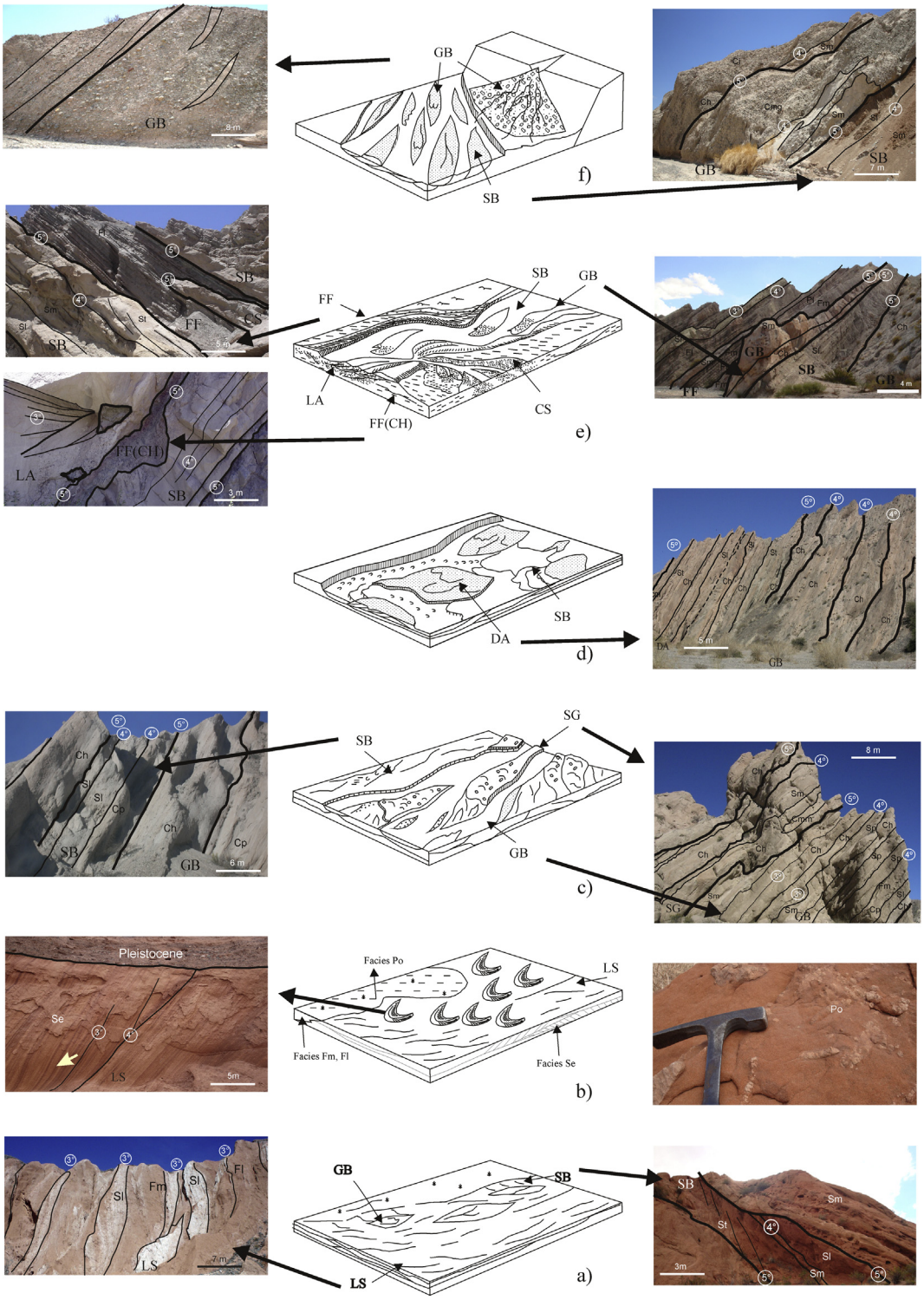

Fig. 8. Description of the paleoenvironment with architectural elements illustrated using schematic diagrams and photos of the Payogastilla Group. a) Fluvial system of the Los Colorados Formation, LAST (Sequence II), proximal ephemeral confined (SB element) in the base, b) unconfined ephemeral – mud flat (LS element) associated with wind deposits (HAST), c) Gravel-bed braided river system associated with gravity flow deposits, Angastaco Formation of the middle part of the deposits with its architectural elements, d) Deep gravel-bed braided river at the top Angastaco Formation, with its architectural elements, e) meandering fluvial sand-gravel system with small lakes of the Palo Pintado Formation with its architectural elements, and f) braided fluvial fan and river system of San Felipe Formation with its architectural elements.

western basin; in the eastern part of the study area (Tonco Sur profile), however, slates, phyllites, and schists from the Puncoviscana Formation are present. There are fewer paleovolcanic clasts from the Eruptive Belt of the Eastern Puna (Calchaquí River) and neovolcanics in the San Lucas River and the Tonco Sur area, which are associated with paleocurrent directions from the northwest and west. In the area of San Lucas and the Tonco Sur River, a small but significant component of the red sandstone clasts from the Lumbrera Formation and gray sandstones of the Maíz Gordo Formation represent the Salta Group. These data

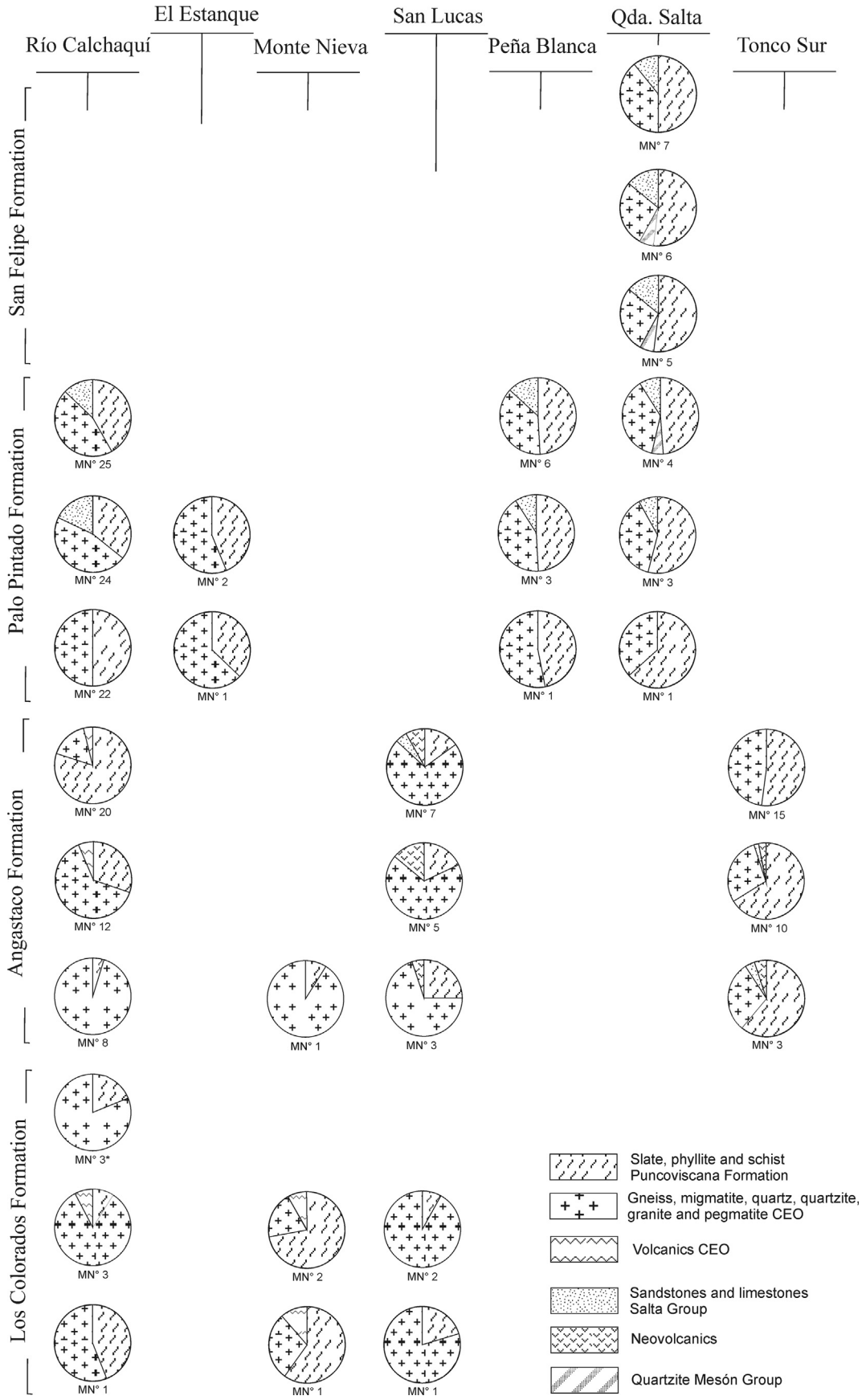

Fig. 9. Percentage of conglomerate clasts from the Payogastilla Group.

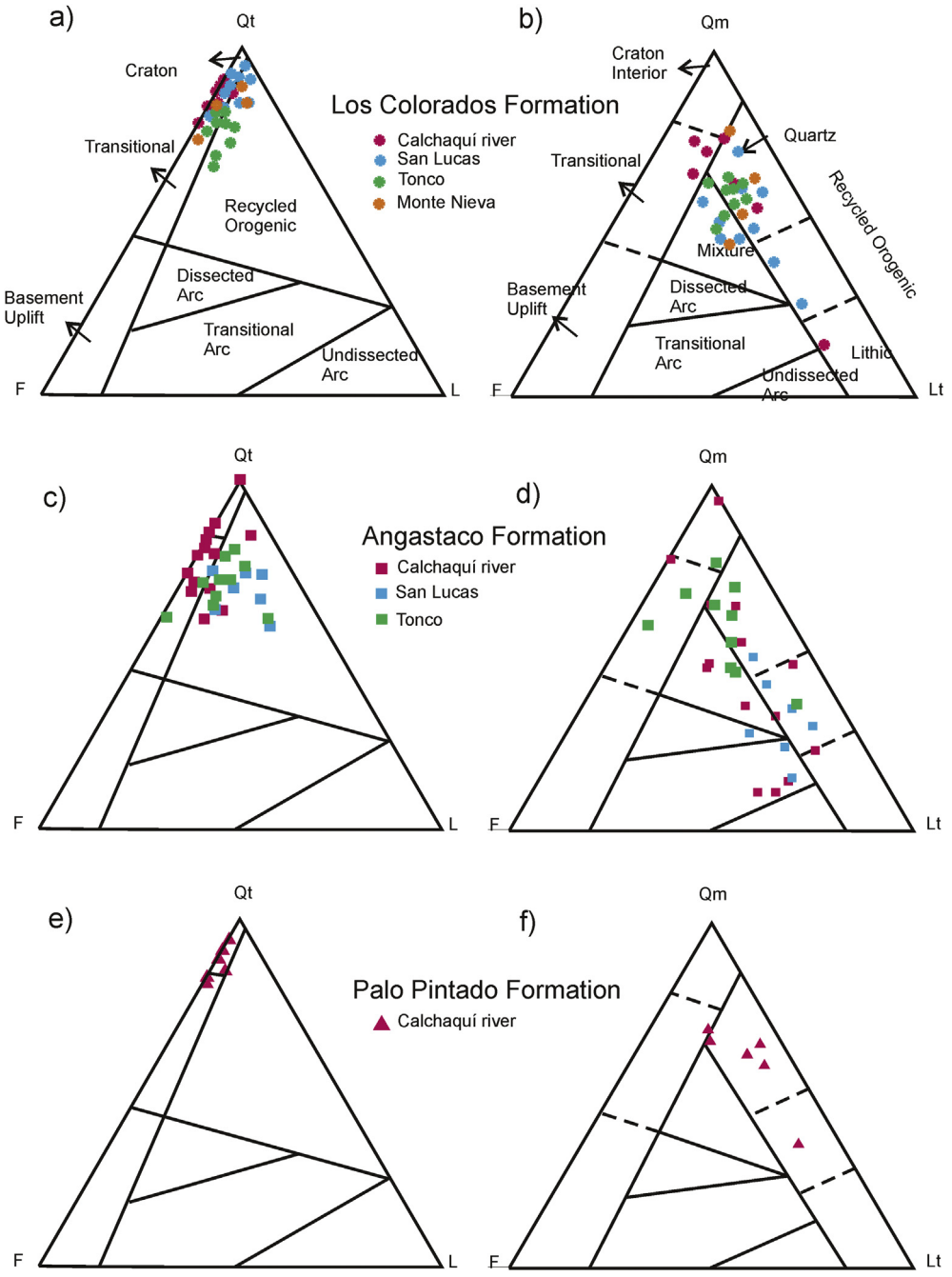

Fig. 10. QtFL and QmFLt diagrams discriminating the provenance of sandstones from the Los Colorados Formation in which there is a high concentration in the Interior Cratonic and Continental Transition fields (a) and some displacement towards Recycled Orogen (b). Angastaco Formation sandstones show some concentration in the Recycled Orogen field (c) and high dispersion in various fields (d). Palo Pintado Formation sandstones with a projection similar to that of the basal unit (e and f) (after Dickinson, 1985).

suggest the tectonic uplift of the Sierra León Muerto in the eastern study area (Fig. 1).

Clast counts in the Palo Pintado Formation, whose outcrops are rare in the southern Calchaquí Valley, show a constant prevalence of pebbles from the Puncoviscana Formation and the Complejo Eruptivo Oire. The middle and upper portions of the unit contain red Salta Group sandstone clasts and pink quartzites, some with Skolithos from the Mesón Group (upper Cambrian).

The origin of the conglomerate in the San Felipe Formation was analyzed in the Quebrada Salta, which also contains elements of the Puncoviscana Formation and the Complejo Eruptivo Oire. The conglomerate also contains limestone clasts from the Yacoraite Formation (Salta Group) and conglomeratic clasts from the Pirgua Subgroup (Salta Group), which are associated with paleocurrent directions from the west and southwest (Fig. 4).

5.2. Petrographic components of the sandstones

The sandstone facies of the Payogastilla Group consist of quartz and lithic sandstones and smaller amounts of coarse- to very coarse-grained feldspathic sandstones (Pettijohn et al., 1973) (Figs. 10 and 11, Table 6).

Quartz is the major component and occurs as mono- and polycrystalline grains (Fig. 11). The facies contain large quantities

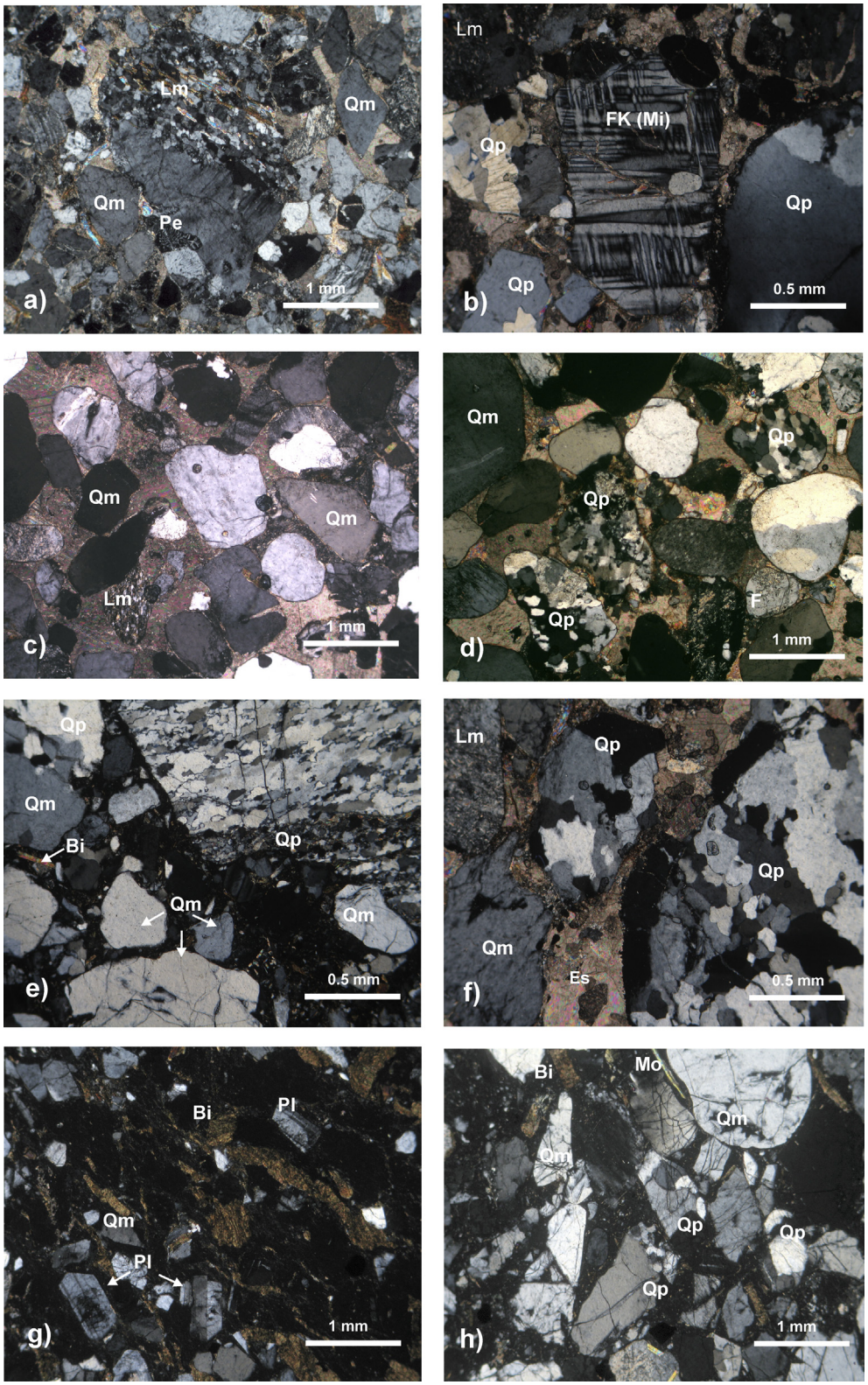

Fig. 11. Photomicrographs of sandstones from the Payogastilla Group (crossed Nicols). a, b, c and d) Los Colorados Formation sandstones (c and d aeolian sandstones) showing the following: polycrystalline quartz (Qp), monocrystalline quartz (Qm), potassium feldspars (FK) and metamorphic lithic fragments (Lm); e and f) Angastaco Formation sandstone showing: polycrystalline quartz (Qp), monocrystalline quartz (Qm), metamorphic lithic fragments (Lm) and biotite (Bi); g) a Palo Pintado Formation tuff, biotite (Bi), plagioclase (Pl), sporadic quartz (Qm) and microcrystalline kaolinitic matrix; and h) Palo Pintado Formation sandstone showing well-rounded and angular (Qm and Qp) grains of quartz, biotite (Bi), and muscovite (Mo) with a calcium carbonate cement.

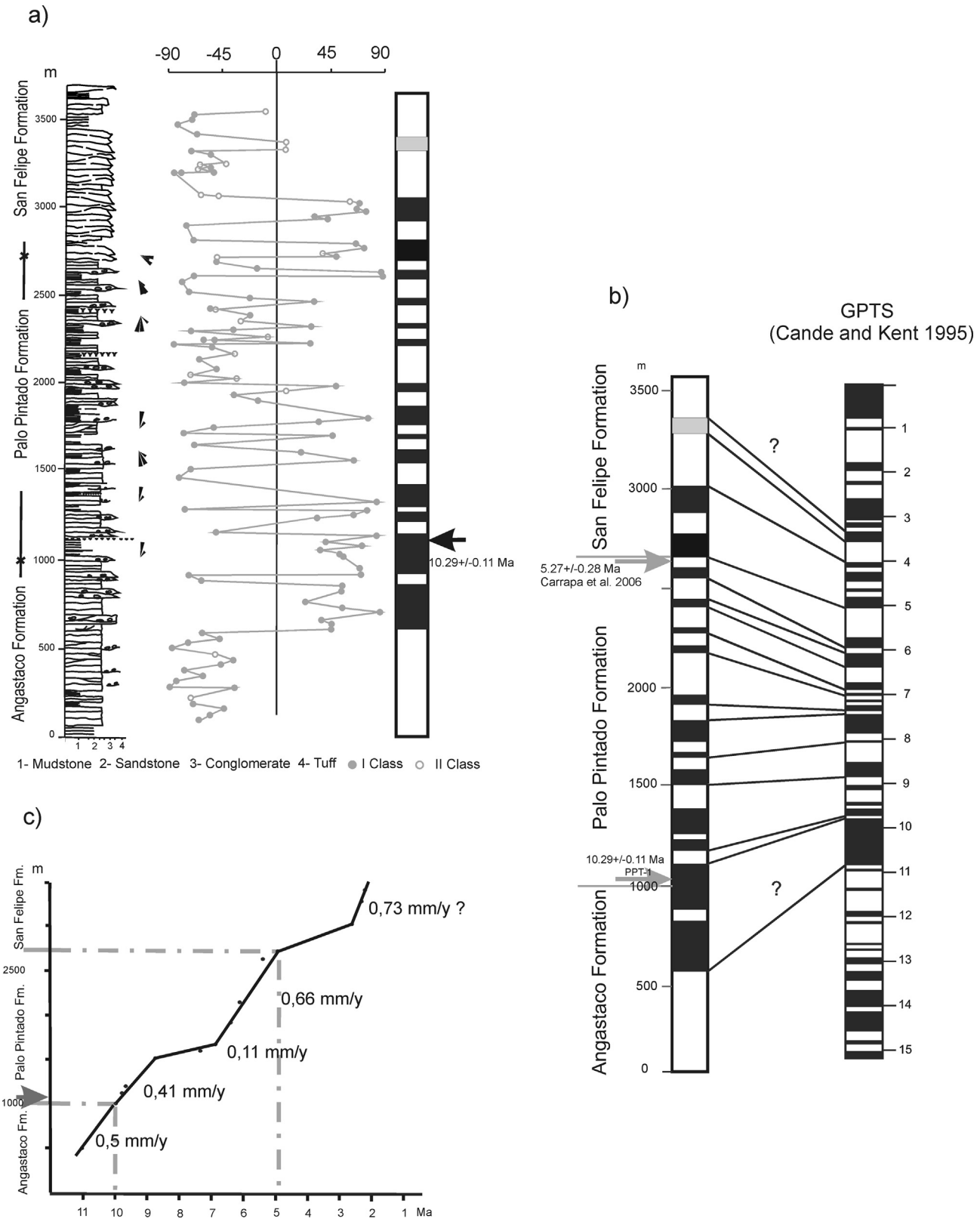

Fig. 12. a) Correlation of the Palo Pintado Formation stratigraphic column vs. the local magnetostratigraphic column (Calchaquí river) showing the Virtual Magnetic Pole latitudes (VGP) vs. stratigraphic level. b) Global Magnetic Polarity Time Scale (GMPTS, Cande and Kent, 1995). c) Sediment accumulation rate in the Palo Pintado Formation, in the Río Calchaquí.

Table 6
Sandstone grain compositions normalized to 100%. Qt: total quartz, F: feldspars, L: lithic fragments, Qm: monocrystalline quartz, Lt: lithic fragments + polycrystalline quartz, Lm: metamorphic lithic fragments, Lv: volcanic lithic fragments, Lp: plutonic lithic fragments.

Location	Formation	Sample	Qt	F	L	Qm	F	Lt
		LC-1	83,5	14	2,5	62	14	24
		LC-3a	87	9	4	16	16	72
	Los	LC-3b	87	13	0	64	14	12
		LC-3c	78	22	0	65	22	13
	Colorados	LC-3d	82,5	17,5	0	74	18	8
		LC-3e	89	11	0	55	11	34
		LC-3f	90	10	0	75	10	15
		C-A-1a	99	1	0	95	1	4
Calchaquí		C-A-1b	77,5	18,5	12,3	33	18	49
	Angastaco	C-A-1c	70	27	3	48	27	25
		C-A-1c'	87	13	0	23	13	64
		C-A-2a	59	30	11	10	30	50
		C-A-6	61,5	24,5	14	14,5	24,5	61
		C-A-7	62,3	27,8	0,9	7,3	27,8	64,4
		C-A- 8	64,2	15,3	20,5	44,2	15,3	40,5
		C-A- 9	62,1	30	7,9	10,5	30	59,5
		C-A- 10	74,4	10,5	15,1	54,4	10,5	35,1
		C-A- 11	69,2	9,7	21,1	49,2	9,7	41,1
River		C-A- 12	62,2	17,3	20,5	42,2	17,3	40,5
		A- 13	79,2	8,5	12,3	64,2	8,5	27,3
		A- 14	77,1	18,3	4,6	47,6	18,3	34,1
		C-PP-1	80,5	16,8	2,7	64,5	16,8	18,7
		C-PP-2	91,5	8,5	0	57	8,5	34,5
	Palo	C-PP-3	94	6	0	64	6	30
		C-PP-4	89	11	0	35	11	54
	Pintado	C-PP-5	83	17	0	68	17	15
		C-PP-6	86	11	3	61	11	28
		SL-LC-1	85,5	12	2,5	62	12	26
		SL-LC-2	89,2	7,2	3,6	16,7	7,2	76,1
	Los	SL-LC-3	83,5	16,5	0	64	16,5	19,5
		SL-LC-4	77,6	20	2,4	65	20	15
		SL-LC-5	82,5	17,5	0	74	18	8
San	Colorados	SL-LC-6	89	11	0	55	11	34
		SL-LC-7	83,2	11,7	5,1	72	11,7	16,3
		SL-A-1	71,5	18,5	28,5	32,5	18,5	49
Lucas		SL-A-2	70	17	13	48	17	35
		SL-A-3	80	13	7	23	13	64
	Angastaco	SL-A-4	53,5	12	34,5	18,6	12	69,4
		SL-A-5	61,5	14,5	24	24,5	14,5	61
		SL-A-6	62,3	27,8	0,9	7,3	27,8	64,4
		SL-A-7	64,2	15,3	20,5	44,2	15,3	40,5
		T-LC-1	73,5	24	2,5	52	24	24
		T-LC-2	57	19	24	16	19	65
		T-LC-3	71,2	16,5	12,3	64	16,5	19,5
	Los	T-LC-4	68	22	11,5	54,6	22	23,4
		T-LC-5	80	17,5	2,5	74	17,5	8,5
		T-LC-6	79	21	14,4	45	21	34
	Colorados	T-LC-7	72	18,3	9,7	52	18,3	29,7
		T-LC-8	73,2	16,4	10,4	37,4	16,4	46,2
Tonco		T-LC-9	76,8	18,1	5,1	39,2	18,1	42,7
		T-A-1	69,8	29,5	0,7	32,6	29,5	37,9
		T-A-2	69,5	6,5	24	44,5	6,5	49
		T-A-3	69	16	15	48	15	37
		T-A-4	80	13	7	23	13	64
	Angastaco	T-A-5	63,5	2	34,5	18,6	2	79,4
		T-A-6	69,5	16,5	14	22,5	16,5	61
		T-A-7	64,3	17,5	18,2	38,1	17,5	44,4
		T-A-8	64,2	15,3	20,5	44,2	15,3	40,5
		T-A-9	71,8	0,9	27,3	60,4	0,9	38,7
		T-A-10	76,1	2	21,9	59,3	2	38,7
		MN-LC-1	89,7	10	0,3	45,3	10	44,7
Monte	Los	MN-LC-2	87,7	9,7	2,6	74,8	9,7	15,5
Nieva	Colorados	MN-LC-3	64,3	7,9	27,8	54,3	7,9	37,8
		MN-LC-4	90,5	4,2	5,3	70,2	4,2	25,6

of clear and undulose monocrystalline quartz of plutonic origin (Fig. 11 a, b, c, e, f, and h) and a smaller proportion of low-grade and polycrystalline quartz, comprising more than three elements per grain, with both crenulated contacts (metamorphic origin; Fig. 11 d, e, and f) and straight contacts (plutonic origin; Fig. 11 b, d, and h).

Feldspars make up a low percentage of the sandstones. Potassium feldspars (FK) and plagioclase feldspars (P) can be distinguished. The potassium feldspars are orthoclase with high kaolinization and fresh microcline (Fig. 11) in round to subrounded grains. In general, the plagioclase has a perthitic texture and forms aggregates with a graphic texture (plutonic origin) (Fig. 11a).

The lithic component is composed of metamorphic clasts (schists, phyllites, and slates) with variable percentages and a few volcanic and sedimentary fragments.

In the Qt-F-L diagram (Fig. 10), the samples are concentrated in the internal craton and continental transition areas. The samples are more dispersed in the Qm-F-Lt diagram (Fig. 9), which suggests variable origins along the column. The Los Colorados Formation sandstones indicate a continental transition, a quartz recycled orogen, and a lithic recycled orogen. The Angastaco Formation represents a recycled orogen that is mixed and transitional, and the Palo Pintado Formation represents a recycled orogen.

The paleocurrent directions of the Payogastilla Group change from the base to the top of the column. The paleocurrents are from the southwest and south in the Los Colorados Formation, from the west, southeast, and northwest in the Angastaco Formation, and from the southwest and northwest in the Palo Pintado Formation.

6. Age of the Payogastilla Group deposits

To improve the stratigraphic correlations in the study area, three airfall beds from the Angastaco Formation and two airfall deposits from the Palo Pintado Formation were selected for the U–Pb analysis of zircon grains. Additionally, two sandstone samples from the Los Colorados Formation were collected for U–Pb zircon provenance ages (in Quebrada Los Colorados). The obtained data are listed in Tables 3 and 4.

6.1. Angastaco Formation

Sample 1 LC-A, from the Calchaquí River sections, was collected at the base of the Angastaco Formation in the Los Colorados River (Calchaquí River profile, Tuff 1 in Fig. 5) and had a U–Pb zircon age of 13.6 ± 0.1 Ma (Fig. 6a). Sample 20, from the Tonco section, was collected from the middle part of the Angastaco Formation in the Tonco Valley (Tuff 7 in Fig. 5) and had a U–Pb zircon age of 13.7 ± 0.1 Ma (Fig. 6b). Finally, the sample 1A from the Amblayo section was obtained from the middle part of the Angastaco Formation in the Amblayo Valley (Tuff 8 in Fig. 5) and had a U–Pb zircon age of 13.7 ± 0.1 Ma (Fig. 6c). Because the three ages overlap and are within the analytical error, the ages can be considered the same.

Sample 1 LC-A, from the same level, was dated at 15.26 ± 0.23 Ma U–Pb by Pereyra et al. (2008) and is from the base of the Angastaco Formation near the contact with the Los Colorados Formation.

6.2. Palo Pintado Formation

Two airfall deposits (samples 2 PP and 1 PP, from the Palo Pintado Formation in the Quebrada El Estanque section) (Fig. 6d) had U–Pb ages of 6.8 ± 0.1 Ma and 6.3 ± 0.1 Ma respectively (Fig. 6e).

6.3. Los Colorados Formation

Two Los Colorados Formation samples collected for U–Pb provenance ages (in Quebrada Los Colorados) were also analyzed. Sample Payo-3 was from very coarse sandstone at the base of the formation, and sample Payo-2 was from sandstone at the top. Seventy-five U–Pb analyses were performed on single grains from sample Payo-3 (Table 4, Fig. 7). The zircon grains are small, up to 300 μm in length, and prismatic with common inclusions. The data define a unimodal zircon distribution (Fig. 7) in which the main population crystallized between 429 and 568 Ma (87% of the grains) with a mean peak at 483 Ma. Minor peaks at 520, 536 and 556 Ma were also observed. Scattered zircons (13% of the grains) with ages between 600 and 1500 Ma were also observed. No Cenozoic zircon ages were found in this sample. Sixty-nine U–Pb analyses were performed on single grains from the upper part of Los Colorados Formation (sample Payo-2; Table 4, Fig. 7). The zircon grains are small, up to 200 μm in length, and prismatic to round. The data define a unimodal zircon distribution (Fig. 7) in which the main population crystallized between 398 and 689 Ma (81% of the grains); this distribution includes a main peak at 468 Ma and minor peaks at 402, 532, 555 and 601 Ma. A small Mesoproterozoic/Neoproterozoic boundary zircon population with ages between 879 and 1019 Ma (10% of the grains) has a peak at 986 Ma. Neoproterozoic (~780 Ma), Mesoproterozoic (1398 Ma), and Paleoproterozoic (not shown) scattered zircons (9% of the grains) are also present. Only one Cenozoic zircon (19 Ma) was found. This date is interpreted as the maximum depositional age of the formation.

In the Calchaquí River, a paleomagnetic study was performed on the entire 5000 m thick Payogastilla Group. However, results were only obtained for 3500 m of the sequence, which includes the upper section of the Angastaco Formation, the Palo Pintado Formation (1850 m), and the base of the San Felipe Formation (Fig. 12a).

Two tuff levels, one at the base of the Palo Pintado Formation that was dated at 10.20 ± 0.11 Ma (Galli et al., 2008) and another at the contact with the San Felipe Formation that was dated at 5.27 ± 0.28 Ma (Coutand et al., 2006), are used to correlate the local magnetic stratigraphic column with the global polarity time scale (Fig. 12 b; GPTS, Cande and Kent, 1995). The paleomagnetic results provide very high-quality data for the Palo Pintado Formation deposits, all of which are Class I data; thus a plot of the stratigraphic levels as a function of the ages (Fig. 12c) indicates that the sediment accumulation rate at the base of the deposits is 0.4 mm/year. This rate decreases to 0.11 mm/year between 8.8 and 6.9 Ma and increases to 0.66 mm/year in the upper third of the deposits to 4.9 Ma (Fig. 12c). The sediment accumulation rate in the upper third of the deposits increases when the red sandstone clasts of the Salta Group appear in the Palo Pintado Formation (Fig. 12c).

A third tuff level is present in the San Felipe Formation and is dated at 5.17 ± 0.23 Ma. This level is located ~135 m above the contact with the Palo Pintado Formation (Bywater Reyes et al., 2010).

7. Discussion

The Payogastilla Group is a relatively well-dated foreland basin deposit that was clearly controlled by tectonics and climate. Based on the observed stratigraphic relationships as well as the paleoenvironment, provenance, paleocurrenst, and age characteristics, we infer substantial tectonic and climatic changes in the stratigraphic record from the Eocene to the Pliocene.

In conjunction with the isotopic ages reported by other authors for the Lumbrera Formation II and the Los Colorados Formation, we conclude that the ages of 47.7 ± 7 Ma (U–Pb) and 40 ± 0.6 Ma (detrital zircons of Monte Nieva) are from deposits located beneath the base of the Los Colorados Formation in the Lumbrera Formation. These ages are consistent with the age of 39.9 ± 0.4 Ma (U–Pb) proposed by del Papa et al. (2010) for the top of the Lumbrera Formation.

A clear paraconformity is located between the Lumbrera Formation II and the Los Colorados Formation. This paraconformity is similar to those observed in older deposits outside the study area (Luracatao and Pucará Valleys; del Papa et al., 2010; Hongn et al., 2007, 2008, 2010 a; b; Payrola Bossio et al., 2009, 2010). Similarly, a paraconformity at the upper contact of the Los Colorados

Formation with the Angastaco Formation is clearly visible in the Calchaquí River, Monte Nieva, San Lucas, and Amblayo. The contact is an unconformity in Tonco Valley (Fig. 3) but does not have a transitional relationship, in contrast to what DeCelles et al. (2011) and Carrapa et al. (2011, 2012) proposed. The Pucará and Luracatao basins had been isolated from the Angastaco basin since the deposition of the Salta Group (Salfity and Marquilas, 1994; Hongn and Seggiaro, 2001). Cerro Negro and Cerro Runo already expressed positive relief during the deposition of the Los Colorados Formation, as was demonstrated by the associated provenance analysis and the indicated paleocurrent directions from the northwest, west, and southwest.

Based on the fossil record, the initial development of the foreland basin, at least in the Luracatao Valley, occurred during the middle Eocene (Payrola Bosio et al., 2009).

Sedimentary filling of the basin began with the deposition of the Los Colorados Formation and was characterized by sheetflood ephemeral fluvial deposits formed by unconfined and confined channels within dune fields in an arid region. In some parts of the basin, aeolian deposits alternate with ephemeral fluvial systems, such as those in the Tonco Valley (Sequences I and III), and cannot be related to the braided fluvial deposits of the overlying Angastaco Formation.

The 19 Ma age of the youngest zircon obtained in this study at the top of the Los Colorados Formation (Payo-2) is consistent with the previous ages obtained by other authors. The 37.6 ± 1.2 Ma age from the base of the Los Colorados Formation in the Pucará basin, the 28.7 ± 1.9 Ma age from detrital apatites in aeolian deposits in the Monte Nieva (DeCelles et al., 2011; Carrapa et al., 2011, 2012), and the 21 ± 0.8 Ma age from the tuff in the aeolian deposits indicate an age range for the deposition of the Los Colorados Formation between the upper Eocene and the lower Miocene. These ages suggest a long deposition interval for the Los Colorados Formation between approximately 35 Ma and at least 19 Ma.

The two sedimentary samples analyzed in Quebrada Los Colorados provide a detrital zircon age dominated by Ordovician components (~87% of the grains; Fig. 7) with a main peak at 483 Ma for the base of Los Colorados Formation (sample Payo-3) and a main peak at 468 Ma for the top of the Los Colorados Formation (sample Payo-2). Considering the depositional age range for the Los Colorados Formation, the U–Pb zircon provenance data indicate that between 35 and 19 Ma, the main provenance area was the Famatinian Magmatic Arc, which is located to the west of this Cenozoic sedimentary basin.

The presence of minor peaks at 520, ~533, and ~555 Ma indicate a provenance from the Pampean Arc and from the Puncoviscana Formation (Lork et al., 1990; Adams et al., 2008; Hauser et al., 2011). The older zircon populations recorded in the two samples reflect the reworking of the Neoproterozoic to lower Paleozoic Eastern Cordillera basement of northwestern Argentina (Hauser et al., 2011). The youngest zircon, which was collected from the top of Los Colorados Formation and had an age of 19 Ma, most likely reflects the contribution of the volcanism from the Miocene arc to the west of the basin (Kay and Coira, 2009).

The onset of basin subsidence was consistent and resulted in constant sediment thicknesses in the study area that increased to the north in the Escoipe region outside the study area. The provenance areas include the Puncoviscana Formation and the Oire Eruptive Complex, which are substantiated by the paleocurrents from the southwest (Sierra Quilmes), west, and northwest (eastern Puna border). These results marked the resumption of the uplift of the adjacent areas during the middle Eocene and Oligocene.

The uplift of the margins of the basin and the renewed relief is reflected in three depositional sequences that are interpreted to represent three tectonic episodes. The beginning of each episode generated accommodation space that was occupied by ephemeral fluvial systems with confined channels (represented by LAST) and paleocurrents from the south and west. Each period of uplift was followed by periods of tectonic inactivity in which the aeolian dune fields, waning flood deposits, and calcic paleosols were deposited (HAST). Consequently, the main controls over the type of fluvial system result from the interactions between tectonics and basin subsidence and the constant arid climatic conditions. We assume that the hiatus in each sequence is significant due to the long time interval represented by the Los Colorados Formation.

The overlying Angastaco Formation has a paraconformity in some areas (Monte Nieva, Calchaquí, San Lucas, and Amblayo Rivers) and an unconformity in other sections (northern and southern Tonco). The age of initial sediment accumulation varies in different parts of the basin. In the Angastaco area, the airfall date indicates an age of 13.6 ± 0.1 Ma (Calchaquí River profile). In other locations, the onset of deposition was dated at >13.5 Ma (sample 20, located ~900 m from the base with a U–Pb age of 13.7 ± 0.1 Ma, and sample 1A, located ~700 m from the base with a U–Pb age of 13.7 ± 0.1 Ma) and <17. 2 Ma (17.2 ± 1.7 Ma U–Pb detrital zircon located ~200 m from the base in Monte Nieva; DeCelles et al., 2011).

The Angastaco Formation consists of a shallow gravel-braided fluvial system at the base that is associated with gravity flow deposits on the basin margins (Calchaquí River). A deep, gravel-braided fluvial system dominates the upper section. Tectonics and subsidence are interpreted as the fundamental controls on the development of the architectural elements of the deposits in the Angastaco Formation, which show changes in the paleoenvironment such as the paleocurrents and the areas of deposition. The paleocurrents measured at the base flowed from the west, northwest, and southwest. In the upper section, the paleoenvironment changes to more erosional rivers with deep channels; the paleocurrents are from the northwest and are associated with neovolcanic clasts from the volcanic-sedimentary sequence of the Almagro-El Toro basin, which has a depositional and eruptive age between 14.3 and 6.4 Ma and synorogenic deposits dated at ~11 Ma (Vezzoli et al., 2012). Red sandstone clasts (Lumbrera Formation) and gray sandstone (Maíz Gordo Formation) in the Tonco Valley are associated with easterly paleocurrents, which suggest a provenance from the uplifted Sierra León Muerto to the east of the Angastaco basin. The Cerro Negro and Cerro Runo Ranges were tectonically reactivated, but the Pucará and Angastaco basins were not separated (Coutand et al., 2006; Carrapa et al., 2011, 2012).

The thickness of the Angastaco Formation varies considerably between the sections in which it is fully exposed (e.g., from 4450 m at the Calchaquí River to 1500 m in the Tonco Valley). The depocenter of the basin between ~13.7 and 10 Ma was in the area of Angastaco.

Although this study did not focus on the structures and the influence of the basement in the region, the accommodation space in this depocenter was clearly influenced by inherited structures (e.g., Cretaceous extensional faults) that were reactivated during Andean compression as high-angle and oblique reverse faults. These structures are located on the western edge of the basin and are similar to those that created local accommodation space in other broken foreland settings (Hongn et al., 2007, 2010 a; b; Iaffa et al., 2011, 2013; Hain et al., 2011; Strecker et al., 2012).

The Palo Pintado Formation was deposited between 10 Ma and 5 Ma. During this interval, the fluvial system was not connected to the sea. The geometry and the fluvial architectural characteristics are a direct consequence of allogenic controls, such as tectonic activity, under constant climatic conditions. The Palo

Pintado Formation developed in a wet tropical climate as a sinuous sandy-gravel fluvial system with swamps and lagoons. During the upper Miocene, the uplift of the basin caused an increase in the A/D (sedimentary accommodation/deposition) rate, which was also associated with a change in the petrologic composition of the deposits (Galli et al., 2011-a and b). The resulting orographic barriers produced a warmer and wetter climate (Starck and Vergani, 1996; Starck and Anzotegui, 2001). The paleomagnetic analysis reflects the increase in the sedimentation rate from 0.41 mm/year at the base to 0.66 mm/year in the upper third of the sequence, which is associated with a higher percentage of Salta Group clasts. Paleocurrents from the south to the southeast indicate the tectonic reactivation of the deposition area from the Sierra León Muerto (and its continuation to the north as the Sierra Los Colorados). Bywater-Reyes et al. (2010) inferred the exhumation and uplift of the Sierra Los Colorados to have occurred at ~4 Ma based on the first appearance of sedimentary grains. In contrast, we demonstrate that this exhumation was recorded in the conglomerates of the Angastaco Formation. In addition, (U–Th)/He dating indicates that the initial exhumation of the Sierra Los Colorados might have started at ~9 Ma (Carrapa et al., 2011).

In the Quebrada Salta, quartzite clasts with Skolites from the Mesón Group (upper Cambrian) and paleocurrents from the north to the northeast suggest a provenance from Quebrada El Toro, where the Mesón Group is exposed.

At approximately 5 Ma, the Angastaco basin may have separated from the rest of the Cenozoic foreland basin. The San Felipe Formation is characterized by architectural elements of a braided fluvial fan and a shallow gravel-braided fluvial system. It is also characterized by the sudden appearance of conglomerates that contain clasts of different levels of Salta Group deposits, such as typical conglomerates from the Pirgua Subgroup and limestones from the Yacoraite Formation (Balbuena Subgroup); these deposits are associated with paleocurrents from the northeast, east, and southeast. This pattern suggests the reactivation of the Sierra León Muerto and the Sierra Los Colorados in the depositional area.

8. Conclusions

1. The relation between the Lumbrera Formation II (top of the Salta Group) and the Los Colorados Formation (base of the Payogastilla Group) is a clear paraconformity. Deposits of the Los Colorados Formation are defined by an ephemeral river system that is associated with dune fields and calcic paleosols. These deposits comprise three depositional sequences that are bounded by erosion surfaces or sharp facies changes. The lower and upper bounding surfaces are second-order subaerial unconformities (northern and southern Tonco Valley, Amblayo Valley). The estimated age of the Los Colorados Formation, which contains several sequence surfaces, is between the upper Eocene and the lower Miocene. The provenance of these deposits is dominated by Precambrian and Ordovician basement located to the south and west of the basin.
2. The contact between the Los Colorados and Angastaco Formations in the study area is a paraconformity in some locations (Monte Nieva, Calchaquí, San Lucas, and Amblayo rivers) and an unconformity in other locations (northern and southern Tonco). The age of initial deposition varies across the basin but is ~14 Ma in this part of the basin.
3. The base of the Angastaco Formation comprises a shallow gravel-braided fluvial system that is associated with gravity-flow deposits on the basin margins (Calchaquí River). The upper section is dominated by a deep gravel-braided fluvial system. Tectonics and subsidence were the fundamental controls on the evolution of the fluvial style, thickness, and paleocurrent variability. The red sandstone clasts (Lumbrera Formation) and gray sandstone (Maíz Gordo Formation) in the Tonco Valley, which are associated with easterly paleocurrents, suggest that the Sierra León Muerto to the east of the Angastaco basin was uplifted. The Cerro Negro and Cerro Runo Range were tectonically reactivated at that time.
4. From 10 to 5 Ma, the southern part of the basin experienced at least three episodes of tectonic reactivation, which are reflected in variations in the rate of sedimentation in the Palo Pintado Formation. The paleomagnetic analysis reflects the increase in the sedimentation rate from 0.41 mm/year at the base to 0.66 mm/year in the upper third of the formation, which is associated with a higher percentage of Salta Group clasts. Paleocurrents from the south to the southeast indicate tectonic reactivation of the depositional area from the Sierra León Muerto-Sierra Los Colorados. The presence of the Meson Group clasts and paleocurrents from the north and northeast suggest a provenance from the Quebrada El Toro, where the Meson Group outcrops, and suggest a regional north – south slope for the river system.
5. The San Felipe Formation is characterized by architectural elements of a braided fluvial fan and a shallow gravel-braided fluvial system. The provenance and abundant clasts in different levels of the Salta Group, and the association with paleocurrents from the northeast, east, and southeast, suggest a reactivation of the Sierra León Muerto and the Sierra Los Colorados in the depositional area.
6. The Payogastilla Group is represented by several fluvial systems that accumulated within the foreland basin. These fluvial systems in the Los Colorados Formation are composed of three third-order depositional sequences that are separated by prominent subaerial unconformities. The Angastaco Formation and the Palo Pintado Formation each contain three fluvial cycles, and the San Felipe Formation contains at least two cycles. The stratigraphic architecture is mainly controlled by tectonic events, such as the reactivation of the provenance areas (to the west, south, and northwest) and the uplift of new provenance areas (to the east and southeast).

Acknowledgments

This research was funded by the Consejo Nacional de Investigaciones Científicas y Técnicas (CONICET-PIP 2010-2012 – 11220090100-298), UNJu (SECTER 08/E036 and 08/E037), and UNSa (CI-UNSa 1858). We thank Alejandro Pérez for their invaluable comments in the field, Silvia Rosas and Claudio Colarich for their assistance with the graphics and layout, and Roberto Liquin and Paulino Cachizumba for their support of the laboratory work. The authors appreciate and acknowledge to the reviewers for their constructive and positive reviews.

References

Aceñolaza, F.G., Toselli, A., 1976. Consideraciones estratigráficas y tectónicas sobre el Paleozoico inferior del Noroeste Argentino, 2. Actas 2° Congreso Latinoamericano de Geología, Caracas, pp. 755–763.

Adams, C.J., Miller, H., Toselli, A.J., Griffin, W., 2008. The Puncoviscana Formation of northwest Argentina: U–Pb geochronology of detrital zircons and Rb–Sr metamorphic ages and their bearing on its stratigraphic age, sediment provenance and tectonic setting. Neues Jahrb. für Geol. Paläontologie – Abh. Stuttg. 247 (3), 341–352.

Alonso, R.N., Jordan, T.E., Tabbutt, K., Vandervoort, D., 1991. Giant Evaporite Belts of the Neogene Central Andes. Geology 19, 401–404.

Babot, M.J., Powell, J.E., De Muizon, C., 2002. Callistoe vincei, a new Proborhyaenidae (Borhyaenoidea, Metatheria, Mammalia) from the Early Eocene of Argentina. Geobios 35, 615–629.

Bona, P., Starck, D., Galli, C.I., Gasparini, Z., Reguero, M., 2011. Registro de Caiman cf. C. latirostris (Alligatoridae, Caimaninae) en el Mioceno tardío en el Noroeste Argentino. Reunión Anual de la Asociación Paleontológica Argentina, Lujan, Buenos Aires. Argentina, p. 20.

Bona, P., Starck, D., Galli, C., Gasparini, Z., Reguero, M., 2013. Caiman cf. *Latirostris* (Alligatoridae, Caimaninae) in the late Miocene Palo Pintado Formation, Salta province, Argentina: paleogeographic and paleoenvironmental considerations. Ameghiniana 51 (1), 26–36 [Online].

Bond, M., Lopez, G., 1993. El primer Notohippidae (Mammalia, Notoungulata) de la Formación Lumbrera (Grupo Salta) del noroeste argentino. Consideraciones sobre la sistemática de la familia Notohippidae. Ameghiniana 30, 59–68.

Brackebusch, L., 1883. Estudio sobre la Formación Petrolífera de Jujuy. Acad. Nac. Ciencias Córdoba Boletín 2, 137–184.

Bywater-Reyes, S., Carrapa, B., Clementz, M., Schoenbohm, L., 2010. Effect of late Cenozoic aridification on sedimentation in the Eastern Cordillera of northwest Argentina (Angastaco basin). Geology 38, 235–238.

Cande, S.C., Kent, D.V., 1995. Revised calibration of the geomagnetic polarity timescale for the Late Cretaceous and Cenozoic. J. Geophys. Res. 100, 6093–6095. http://dx.doi.org/10.1029/94JB03098.

Carrapa, B., Bywater-Reyes, S., DeCelles, P.G., Mortimer, E., Gehrels, G.E., 2012. Late Eocene–Pliocene basin evolution in the Eastern Cordillera of northwestern Argentina (25°–26°S): regional implications for Andean orogenic wedge development. Basin Res. 24, 249–268. http://dx.doi.org/10.1111/j.1365-2117.2011.00519.x.

Carrapa, B., Trimble, J., Stockli, D., 2011. Patterns and timing of exhumation and deformation in the Eastern Cordillera of NW Argentina revealed by (U–Th)/He thermochronology. Tectonics 30, TC3003. http://dx.doi.org/10.1029/2010TC002707.

Catuneanu, O., 2006. Principles of Sequence Stratigraphy. Elsevier, Amsterdam, p. 375.

Catuneanu, O., Elango, H.N., 2001. Tectonic control on fluvial styles: the Balfour Formation of the Karoo Basin, South Africa. Sediment. Geol. 140, 291–313.

Catuneanu, O., Abreu, V., Bhattacharya, J.P., Blum, M.D., Dalrymple, R.W., Eriksson, P.G., Fielding, Christopher R., Fisher, W.L., Galloway, W.E., Gibling, M.R., Giles, K.A., Holbrook, J.M., Jordan, R., Kendall, C.G., Macurda, B., Martinsen, O.J., Miall, A.D., Neal, J.E., Nummedal, D., Pomar, L., Posamentier, H.W., Pratt, B.R., Sarg, J.F., Shanley, K.W., Steel, R.J., Strasser, A., Tucker, M.E., Winker, C., 2009. Towards the standardization of sequence stratigraphy. Pap. Earth Atmos. Sci., 35. Paper 238. http://digitalcommons.unl.edu/geosciencefacpub/238.

Condie, K.C., 2003. Plate Tectonics and Crustal Evolution, fourth ed. Bookcraft (Bath) Ltd., 294.

Coutand, I., Carrapa, B., Deeken, A., Schmitt, A.K., Sobel, E., Strecker, M.R., 2006. Orogenic plateau formation and lateral growth of compressional basins and ranges: insights from sandstone petrography and detrital apatite fission-track thermochronology in the Angastaco Basin, NW Argentina. Basin Res. 18, 1–26.

DeCelles, P.G., Carrapa, B., Horton, B., Gehrels, G.E., 2011. Cenozoic foreland basin system in the central Andes of northwestern Argentina: implications for Andean geodynamics and modes of deformation. Tectonics 30, TC6013. http://dx.doi.org/10.1029/2011TC002948.

Deeken, A., Sobel, E., Coutand, I., Haschke, M., Riller, U., Strecker, M., 2006. Development of the Southern Eastern Cordillera, NW Argentina, constrained by apatite fission track thermochronology: from Early Cretaceous extension to middle Miocene shortening. Tectonics 25, TC6003. http://dx.doi.org/10.1029/2005TC001894.

del Papa, C.E., Hongn, F.D., Petrinovich, I.A., Dominguez, R., 2004. Evidencias de deformación pre-miocena media asociada al antepaís andino en la Cordillera Oriental (24° 35'S – 66° 12'O). Nota Breve. Rev. la Asoc. Geológica Argent. 59, 506–509.

del Papa, C.E., 2006. Estratigrafía y paleoambientes de la Formación Lumbrera, Grupo Salta, Noroeste Argentino. Rev. la Asoc. Geológica Argent. 61, 313–327.

del Papa, C., Kirschbaum, A., Powell, J., Brod, A., Hongn, F., Pimentel, M., 2010. Sedimentological, geochemical and paleontological insights applied to continental omission surfaces: a new approach for reconstructing an Eocene foreland basin in NW Argentina. J. S. Am. Earth Sci. 29, 327–345.

del Papa, C.E., Hongn, F., Powell, J., Payrola Bosio, P., Do Campo, M., Strecker, M.R., Petrinovic, I., Schmitt, A.K., Pereyra, R., 2013. Middle Eocene-Oligocene broken-foreland evolution in the Andean Calchaqui Valley, NW Argentina: insights from stratigraphic, structural and provenance studies. Basin Res. 25, 1–20. http://dx.doi.org/10.1111/bre.12018.

Diaz, J.I., Malizzia, D.C., 1983. Estudio geológico y sedimentológico del Terciario Superior del valle Calchaquí (departamento de San Carlos, provincia de Salta). Boletín Sedimentológico 2, 8–28.

Dickinson, W.R., 1985. Interpreting provenances relations from detrital models of sandtone. In: Zuffa, G. (Ed.), Provenences of Arenitas, 148. Reidel Publishing Company, Serie, pp. 333–361.

Embry, A.F., 1995. Sequence boundaries and sequence hierarchies: problems and proposals. In: Steel, R.J., Felt, V.L., Johannessen, E.P., Mathieu, C. (Eds.), Sequence Stratigraphy on the Northwest European Margin, pp. 1–11. Special Publication 5, Norwegian Petroleum Society.

Galli, C.I., Ramirez, A., Barrientos, C., Reynolds, J., Viramonte, J.G., Idleman, B., 2008. Estudio de proveniencia de los depósitos del Grupo Payogastilla (Mioceno Medio-Superior) aflorantes en el río Calchaquí, provincia de Salta. Actas 17° Congreso Geológico Argentino, Jujuy, Argentina, pp. 353–354.

Galli, C.I., Ramirez, A., Reynolds, J., Viramonte, J.G., Idleman, B., Barrientos, C., 2011a. Proveniencia de los depósitos del Grupo Payogastilla (Cenozoico), río Calchaquí, provincia de Salta, Argentina. Rev. Asoc. Geológica Argent. 68, 263–278.

Galli, C.I., Anzotegui, L.M., Horn, M.Y., Morton, L.S., 2011b. Paleoambiente y paleocomunidades de la Formación Palo Pintado (Mioceno-Plioceno), Provincia de Salta, Argentina. Rev. Mex. Ciencias Geológicas 28, 161–174.

Galli, C.I., Reynolds, J., 2012. Evolución paleoambiental del Grupo Payogastilla (Eoceno – Plioceno) en el valle Calchaquí – Tonco, provincia de Salta. 13° Reunión Argentina de Sedimentología, Relatorio Salta, Argentina, pp. 67–80.

Gasparini, Z., Fernandez, M., Powell, J., 1993. New Tertiary Sebecosuchians (Crocodylomorpha) from South America: phylogenetic implications. Hist. Biol. 7, 1–19.

Gomez Omil, R.J., Boll, A., Hernadez, R.M., 1989. Cuenca cretácico-terciaria del Noroeste argentino (Grupo Salta). En Cuencas Sedimentarias Argentinas. In: Chebli, G.A., Spalletti, L.A. (Eds.), Universidad Nacional de Tucumán, vol. 6, pp. 43–64. Serie de Correlación Geológica.

Graham, S.A., Tolson, R.B., Decelles, P.G., Ingersoll, R.V., Bargar, E., Caldwell, M., Cavazza, W., Edwards, D.P., Follo, M.F., Handschy, J.F., Lemke, L., Moxton, I., Rice, R., Smith, G.A., White, J., 1986. Provenance modelling as a technique for analysing source terrane evolution and controls on foreland sedimentation. In: Allen, A., Homewood, P. (Eds.), Foreland Basin. Blackwell Scient., Oxford, pp. 425–436.

Grier, M.E., 1990. The Influence of the Cretaceous Salta Rift Basin on the Development of Andean Structural Geometries. University of Cornell, Ithaca, New York, USA, p. 178. NW Argentine Andes. PhD. thesis.

Grier, M.E., Dallmeyer, R.D., 1990. Age of the Payogastilla Group. Implications for foreland basin development, NW Argentina. J. S. Am. Earth 4, 351–372.

Hain, M., Strecker, M., Bookhagen, B., Alonso, R., Pingel, H., Schmitt, A., 2011. Neogene to Quaternary broken foreland formation and sedimentation dynamics in the Andes of northwest Argentina (25°S). Tectonics 30 (1–27), TC2006. http://dx.doi.org/10.1029/2010TC002703.

Hauser, N., Matteini, M., Omarini, R.H., Pimentel, M.M., 2011. Combined U-Pb and Lu-Hf isotope data on turbidites of the Paleozoic basement of NW Argentina and petrology of associated igneous rocks: Implications for the tectonic evolution of western Gondwana between 560 and 460Ma. Gondwana Res. 19, 100–127.

Herbst, R., Anzotegui, L.M., Esteban, G., Mautino, L.R., Morton, S., Nassif, N., 2000. Síntesis paleontológica del Mioceno de los valles Calchaquíes, noroeste argentino, en El Neógeno de Argentina. In: Aceñolaza, F., Herbst, R. (Eds.), Argentina, Instituto Superior de Correlación Geológica, vol. 14, pp. 263–288. Serie Correlación Geológica.

Hongn, F., Seggiaro, R., 2001. Hoja Geológica 2566-III, Cachi. Programa Nac. Cartas Geológicas la República Argent. Boletín 248, 87 escala 1:250.000.

Hongn, F., del Papa, C., Powell, J., Petrinovic, I., Mon, R., Deraco, V., 2007. Middle Eocene deformation and sedimentation in the Puna-Eastern Cordillera transition (23°–26° S): control by preexisting heterogeneities on the pattern of initial Andean shortening. Geology 35, 271–274.

Hongn, F., del Papa, C., Powell, J., Petrinovic, I., Mon, R., 2008. Discordancias en el cerro Tin Tin (Salta): claves para interpretar la evolución tectónica en el noroeste argentino. Actas 17° Congreso Geológico Argentino, Jujuy, pp. 26–27.

Hongn, F., Mon, R., Petrinovic, I., del Papa, C., Powell, J., 2010a. Inversión y reactivación tectónica cretácica cenozoica en el noroeste argentino: Influencia de las heterogeneidades del basamento Neoproterozoico-Paleozoico inferior. Rev. Asoc. Geológica Argent. 66, 38–53.

Hongn, F., del Papa, C., Powell, J., Payrola Bosio, P., Petrinivic, I., Mon, R., 2010b. Fragmented paleogene foreland basin in the Valles Calchaquí, NW of Argentina. In: Salfity, J.A., Marquillas, R.A. (Eds.), Cenozoic Geology of the Central Andes of Argentina. SCS Publisher, pp. 198–210.

Iaffa, D.N., Sàbat, F., Bello, D., Ferrer, O., Mon, R., Gutierrez, A.A., 2011. Tectonic inversion in a segmented foreland basin from extensional to piggy back settings: the Tucumán basin in NW Argentina. J. South Am. Earth Sci. 31, 457–474.

Iaffa, D.N., Sàbat, F., Muñoz, J.A., Carrera, N., 2013. Basin Fragmentation Controlled by Tectonic Inversion and Basement Uplift in Sierras Pampeanas and Santa Bárbara System, Northwest Argentina. Geological Society, London. http://dx.doi.org/10.1144/SP377. Special Publications 377.

Ingersoll, R.I., Bullard, T.F., Ford, R.L., Grimm, J.P., Picle, J.D., Sares, S.W., 1984. The effect of grain size on detrital modes: a test of the Gazzi-Dickinson point-counting method. J. Sediment. Petrol. 54, 103–116.

Jordan, T.E., Alonso, R.N., 1987. Cenozoic stratigraphy and Basin Tectonics of the Andes Mountain, 20–28 South Latitude. Am. Assoc. Petroleum Geol. 71, 49–64. Tulsa.

Kay, S.M., Coira, B., 2009. Shallowing and steepening subduction zones, continental lithospheric loss, magmatism and crustal flow under the Central Andean Altiplano-Puna plateau. In: Kay, S.M., Ramos, V.A., Dickinson, W.R. (Eds.), Backbone of the Americas: Shallow Subduction, Plateau Uplift and Ridge Collision, vol. 204. The Geological Society of America Memoir, pp. 229–258.

Lork, A., Bahlburg, H., 1993. Precise U-Pb ages of monazites from the Faja Eruptiva de la Puna Oriental and the Cordillera Oriental, NW Argentina. Actas 12° Congreso Geológico Argentino y 2° Congreso de Exploración de Hidrocarburos 4, 1–6.

Lork, A., Miller, H., Kramm, U., Grauert, B., 1990. Sistemática U-Pb de circones detríticos de la Formación Puncoviscana y su significado para la edad máxima de sedimentación en la Sierra de Cachi (prov. de Salta, Argentina). In: Aceñolaza, F.G., Miller, H., Toselli, A.J. (Eds.), El Ciclo Pampeano en el Noroeste Argentino. Serie de Correlación Geológica 4. Universidad de Tucumán, pp. 199–208.

Ludwig, K.R., 2003. User's Manual for Isoplot/Ex v. 3.00. A Geochronological Toolkit forMicrosoft Excel, Berkeley, p. 71. BGC Special Publication 4.
Marquillas, R.A., del Papa, C., Sabino, I.F., 2005. Sedimentary aspects and paleoenvironmental evolution of a rift basin: Salta Group (Cretaceous-Paleogene), northwestern Argentina. J. S. Am. Earth Sci. 94, 94–113.
McFadden, P.L., McElhinny, M.W., 1990. Classification of the reversal test in palaeomagnetism. Geophys. J. Int. 103, 725–729.
Miall, A.D., 1985. Architectural-element analysis: a new method of facies analysis applied to fluvial deposits. Earth Sci. Res. J. 22, 261–308.
Miall, A.D., 1994. Reconstructing fluvial macroform architecture from two-dimensional outcrops: examples from the Castlegate Sandstone, Book Cliffs, UTA. J. Sediment. Res. B64, 146–158.
Miall, A.D., 1995. Description and interpretation of fluvial deposits: a critical perspective: discussion. Sedimentology 42, 379–384.
Miall, A.D., 2006. The Geology of Fluvial Deposits. Sedimentary Facies, Basin Analysis and Petroleum Geology. Springer, Berlin, London, p. 581.
Moreno, J.A., 1970. Estratigrafía y paleogeografía del Cretácico superior en la cuenca del noroeste argentino, con especial mención de los Subgrupos Balbuena y Santa Bárbara. Rev. Asoc. Geológica Argent. 25, 9–44.
Omarini, R., Sureda, R., Götze, H., Seilacher, A., Pflüger, F., 1999. Puncoviscana folded belt in northwestern Argentina: testimony of Late Proterozoic Rodinia fragmentation and pre-Gondwana collisional episodes. Int. J. Earth Sci. 88, 76–97.
Pascual, R., 1980. Nuevos y singulares tipos ecológicos de marsupiales extinguidos de América del Sur (Paleoceno tardío o Eoceno Temprano) del noroeste argentino. In: Actas 2° Congreso Argentino de Paleontología y Bioestratigrafía y 1° Congreso Latinoamericano de Paleontología, pp. 151–173. Buenos Aires.
Pascual, R., Bond, M., Vucetich, M., 1981. El Subgrupo Santa Bárbara (Grupo Salta) y sus vertebrados, cronología, paleoambientes y paleobiogeografía. In: Actas 8° Congreso Geológico Argentino, pp. 743–758.
Payrola Bosio, P.P., del Papa, C., Hongn, F.D., Powell, J., 2010. Estratigrafía del Valle de Luracatao (Valle Calchaquí, Noroeste Argentino): nueva propuesta. Rev. Asoc. Geológica Argent. 67, 309–318.
Payrola Bosio, P.P., Powell, J., del Papa, C., Hongn, F., 2009. Middle Eocene deformation-sedimentation in the Luracatao Valley: tracking the beginning of the foreland basin of northwestern Argentina. J. S. Am. Earth Sci. 28, 142–154.
Pereyra, R., Becchio, R., Viramonte, J.G., Pimentel, M., 2008. Minerales pesados en depósitos piroclásticos de caída distales, su uso en la correlación crono-estratigráfica entre la Formación Angastaco (Grupo Payogastilla) y Formación Anta (Grupo Orán). In: Actas 17° Congreso Geológico Argentino, vol. 1, pp. 227–228. Jujuy.
Pettijohn, F., Potter, P.E., Siever, R., 1973. Sand and Sandstones. Springer Verlag, New York, p. 618.
Ramaekers, P., Catuneanu, O., 2004. Development and sequences of the Athabasca basin, Early Proterozoic, Saskatchewan and Alberta, Canada. In: Eriksson, P.G., Atermann, W., Nelson, D.R., Meuller, W.E., Catuneanu, O. (Eds.), The Precambrian Earth: Tempos and Events. Elsevier, Amsterdam, Netherlands, pp. 705–723.
Reyes, F.C., 1972. Correlaciones en el Cretácico de la cuenca Andina de Bolivia, Perú y Chile. Rev. Técnica Y.P.F. Boliv. 1, 101–104.
Reyes, F.C., Salfity, J.A., 1973. Consideraciones sobre la estratigrafía del Cretácico (Subgrupo Pirgua) del noroeste argentino. In: Actas 5° Congreso Geológico Argentino, Carlos Paz, pp. 355–385.
Sabino, I.F., 2004. Estratigrafía de la Formación La Yesera (Cretácico): base del relleno sinrift del Grupo Salta, noroeste argentino. Rev. Asoc. Geológica Argent. 59, 330–340.
Salfity, J.A., Marquilas, R.A., 1994. Tectonic and sedimentary evolution of the Cretaceous-Eocene Salta Group Basin, Argentina. In: Salfity, J.A. (Ed.), Cretaceous Tectonics of the Andes, pp. 266–315. Earth Evolution Sciences, Fried. Vieweg and Sohn, Germany.
Salfity, J.A., Monaldi, C.R., 2006. Hoja Geológica 2566-IV. Metán: Programa Nac. Cartas Geológicas la República Argent. 319, 74 escala 1:250.000.
Schumm, S.C., 1981. Evolution and response of the fluvial system, sedimentologic implication. In: Ethridge, F.G., Flores, R.M. (Eds.), Recent and Ancient Nonmarine Depositional Environments: Models for Exploration. Society Economic Paleontologists Mineralogists, 31, pp. 19–29. Special Publication.
Schumm, S.C., 1985. Patterns of Alluvial rivers. Ann. Rev. Earth Planet. Sci. 13, 5–27.
Starck, D., Anzotegui, L., 2001. The late Miocene climatic change persistence of a climatic Signal through the orogenic stratigraphic record in northwestern of Argentina. J. South Am. Earth Sci. 14, 763–774. http://dx.doi.org/10.1016/S0895-9811(01)00066-9.
Starck, D., Vergani, G., 1996. Desarrollo tecto-sedimentario del Cenozoico en el sur de la Provincia de Salta-Argentina. In: Actas 13° Congreso Geológico Argentino, I, pp. 433–452. Buenos Aires.
Strecker, M.R., Alonso, R.N., Bookhagen, B., Carrapa, B., Hilley, G.E., Sobel, E.R., Trauth, M.H., 2007. Tectonics and climate of the Southern Central Andes. Annu. Rev. Earth Planet. Sci. 35, 747–787. http://dx.doi.org/10.1146/annurev.earth.35.031306.140158.
Strecker, M.R., Hilley, G.E., Bookhagen, B., Sobel, E.R., 2012. Structural, geomorphic, and depositional characteristics of contiguous and broken foreland basins: examples from the eastern flanks of the central Andes in Bolivia and NW Argentina. In: Busby, C., Azor Pérez, A. (Eds.), Tectonics of Sedimentary Basins Recent Advances. Wiley-Blackwell, pp. 508–521.
Toselli, A.J., 1990. Metamorfismo del Ciclo Pampeano. In: Aceñolaza, F.G., Miller, H., Toselli, A.J. (Eds.), El Ciclo Pampeano en el Noroeste Argentino, INSUGEO, vol. 4, pp. 181–197. Serie Correlación Geológica.
Toselli, A.J., Lopez, J.P., Sardi, F.G., 1999. El basamento metamórfico en cumbres Calchaquíes Noroccidentales, Aconquija, Ambato y Ancasti: Sierras Pampeanas. In: González Bonorino, G., Omarini, R., Viramonte, J. (Eds.), Geología del Noroeste Argentino, Relatorio, 19° Congreso Geológico Argentino, pp. 73–79. Salta.
Tunbridge, I.P., 1984. Facies Model for a sandy ephemeral stream and clay playa complex; the Middle Devonian Trentishoe Formation of Noth Devon, U.K. Sedimentology 31, 697–715.
Turner, J.C., 1960. Estratigrafía de la Sierra de Santa Victoria y adyacencias. Acad. Nac. Ciencias Córdoba, Boletín 41 (2), 163–196.
Turner, J.C., Mon, R., 1979. Cordillera Oriental. In: II Simposio de Geología Regional Argentina. Acad. Nac. Ciencias Córdoba 41, 163–169.
Turner, J.C., 1959. Estratigrafía del Cordón de Escaya y Sierra de Rinconada (Jujuy). Rev. Asoc. Geológica Argent 13, 13–59.
Vandervoort, D.S., Jordan, T.E., Zeitler, P.K., Alonso, R., 1995. Chronology of internal drainage development and uplift, southern Puna plateau, Argentine Central Andes. Geology 23, 145–148. http://dx.doi.org/10.1130/0091-7613.
Vezzoli, L., Acocella, V., Omarini, R., Mazzuoli, R., 2012. Miocene sedimentation, volcanismand deformation in the Eastern Cordillera (24°30' S, NW Argentina): tracking the evolution of the foreland basin of the Central Andes. Basin Res. 24, 1–27. http://dx.doi.org/10.1111/j.1365-2117.2012.00547.x.